Application of Magnetic Gradiometry, Magnetic Susceptibility and Electrical Resistivity Tomography in the Characterisation of the Sunyani Municipal Waste Disposal Site

BY

APPIAH ISAAC

BSc. Physics(Hons)

A Thesis Submitted to the Department of Physics, Kwame Nkrumah University of Science and Technology in partial fulfillment of the requirements for the award of the degree

of

MASTER OF PHILOSOPHY (GEOPHYSICS)

Supervisor: Dr. David Dotse Wemegah

College of Science

November, 2016

DECLARATION

I declare that I have wholly undertaken the study reported herein towards the MPhil under the supervision of Dr. D. D. Wemegah and Mr. Van–Dycke Sarpong Asare and that except portions where references have been duly cited, this dissertation to the best of my knowledge contains no material previously published by another person nor material which has been accepted for the award of any other degree of the university.

....	....	....
(Student's name & ID)	Signature	Date

Certified by:

....	....	....
(Supervisor's name)	Signature	Date

Certified by:

....	....	....
(Head of Dept.'s name)	Signature	Date

ACKNOWLEDGEMENTS

I wish to thank and acknowledge the almighty God for his guidance and mercies, once again, through this major milestone in my academic endeavour. My appreciation goes to the Department of Physics which made the Geophysics Laboratory, its facilities and resources available to me at time of the research. I also wish to extend my sincere appreciation and gratitude to my supervisors, Dr. David Dotse Wemegah and Mr. Van–Dycke Sarpong Asare for their painstaking guidance and support. I am grateful to all lecturers at the Department of Physics, Geophysics students of 2016 year group who in one way or the other have contributed to my training. I am thankful to Mr. Owusu Korkor Daniel and Mr. Stephen Asiamah Yeboah, both of the Environmental Health Department of Sunyani Municipal Assembly (SMA) for granting me access and providing other key information about the SMA waste disposal site. My sincere gratitude also goes to my mum, Madam Rose Duah and the rest of the family for their immense support through my academic journey. Last but not the least, I am again indebted to my dear friends Mr. Jerry Lawrence Arthur, Odame Isaac, Kusi–Yeboah Moses, Boadi Benjamin whose immense assistance on the field during the data acquisition and processing stages have brought me this far. I say

God bless you all.

ABSTRACT

Areas that surround unlined solid waste disposal sites depict high tendencies of being contaminated with leachate emanating from the waste deposits that infiltrate into the ground. For that reason, this research seeks to highlight and bring to the attention of city authorities and interest groups the alarming levels of the anthropogenic impact of dumped solid waste on the environment especially, when it pertains to the ground and its water resources using integrated geophysical methods. The integration of three geophysical methods comprising of magnetic gradiometry, magnetic susceptibility and electrical resistivity tomography has helped to characterise the SMA waste disposal site mainly due to the unlined and heterogeneous nature of the waste deposit. The results of both magnetic susceptibility and gradiometric methods displayed in anomaly maps clearly defined the physical boundaries of the waste deposit with an approximate area extent of 82,650 m^2 which is characterised by high magnetic susceptibilities between 426×10^{-5} SI and 9890×10^{-5} SI. Also, an average magnetic intensity value of 32230.74 nT was recorded over the area with values generally greater than the average measured over the main waste body. They also revealed high magnetic anomalies sporadically distributed outside the main waste boundaries which are attributed to indiscriminate deposition and uncontrolled nature of the waste. Similarly, the ERT sections also revealed zones of leachate contamination and accumulation just beneath the waste body and migration pathways for leachate were also delineated with low resistivity signatures up to 43.9 $\Omega.m$. In spite of the success reported herein with the ERT, the research also revealed that the ERT is less effective in estimating the thickness of the waste deposit due to leachate infiltration into the ground beneath it that masks the resistivities of the top level ground and makes it indistinguishable from the waste body. Having estimated an approximate waste thickness of about 5 m using ERT, the volume

of waste expected to be reclaimed from the site for remediation purposes is estimated at 413,250 m^3.

Table of Contents

Figures

Tables

List of Symbols and Acronyms

SMA	Sunyani Municipal Assembly	GPR	Ground Penetrating Radar
EM	Electromagnetic	VLF	Very Low Frequency
MT	Magnetotellurics	SW	Solid Waste
ERI	Electrical Resistivity Imaging	ER	Electrical Resistivity
IP	Induced Polarisation	UST	Underground Storage Tank
MALM	Mise-a-la-masse	HDPE	High Density Poli–ethylene
MSW	Municipal Solid Waste	ZL	Zoomlion
ERT	Electrical Resistivity Tomography	TRM	Thermoremanent magnetisation
WMD	Waste Management Department	DRM	Detrital remanent magnetisation
EPA	Environmental Protection Agency	CRM	Chemical remanent magnetisation
ESP	Environmental Sanitation Policy	VRM	Viscous remanent magnetisation
IRM	Isothermal remanent magnetisation	TMI	Total magnetic intensity
ΔV	Potential difference	θ	Wave number
I_i	Current	π	pi
k	Geometric factor	R	Resistance
a	Potential electrode spacing	∞	infinity
χ_m	Magnetic susceptibility	$\vec{J}_i$	Induced magnetisation vector
$H\sim$	Magnetising field vector	$B\sim$	Magnetic field intensity vector
F	Earth's magnetic field strength	GNI	Gross National Income
f_p	Precession frequency	Φ_p	Gyromagnetic ration
μ_o	Permeability of free space	μ	Permeability of medium
ρ_a	Apparent resistivity	ρ_1	Apparent resistivity of medium 1
ρ_2	Apparent resistivity of medium 2	μ_r	Relative permeability

I	Magnetic inclination	D	Magnetic declination
$L(\theta)$	Reduction to the pole operator	$A(x,y)$	Amplitude of analytic signal
M	Observed total field intensity	RTP	Reduction to the pole
L,a,x	Distance	n	Factor
C_1,C_2	Current electrodes	P_1,P_2	Potential electrodes
A,B	Current electrodes	M,N	Potential electrodes
UTM	Universal traverse mercator	WGS	World geodetic system
GPS	Global positioning system	RF	Radio frequency
BOD_5	Biochemical oxygen demand	COD	Chemical oxygen demand
KNUST	Kwame Nkrumah University of Science and Technology		
MLGRD	Ministry of Local Government and Rural Development		
MMDAs	Metropolitan, Municipal and District Assemblies		
NESPoCC	National Environmental Sanitation Policy Coordinating Council		
DEHMD	District Environmental Health and Management Departments		

Chapter 1

INTRODUCTION

1.1 Background of the Study

Environmental pollution from municipal solid waste (MSW) is a major challenge that city authorities have to contend with in the world today. In many developing and middle–income countries in Africa and Asia, such as Ghana, Nigeria, Liberia, Indonesia etc., the management of MSW is a major drain on the public purse. In the light of lack of capital investment in this sector, inefficient treatment and improper waste management practices such as land–filling and open dumps always characterise the operations of waste managers. The inefficiencies in the management of solid waste (SW) can lead to high pollution levels in the atmosphere, downstream and groundwater systems which undoubtedly have greater tendency of putting public health into serious jeopardy. It is therefore evident that the quality of the air, downstream and groundwater is being compromised by many anthropogenically induced sources and activities such as solid waste disposal (SWD) sites. The situation is further exacerbated when the sites are not engineered leading to the percolation of leachate and infiltration of contaminants through the soil depending on the nature of the immediate underlying rock materials.

Groundwater contamination can be defined as the introduction of any undesirable physical, chemical or micro-organisms into a groundwater source which renders the water unfit for its intended use. These undesirable materials can pose serious threats of polluting the groundwater, downstream surface water resources and soil which eventually expose most people who depend on them to serious health hazards (Wemegah et al., 2014). With a projected daily generation of 109.2 metric tons of municipal solid waste, the people of Sunyani municipality are not immune to the potential threats the contaminants pose to the environment and public health. The chunk of the waste that are generated in the municipality and collected from various collection points are transported to the SMA waste disposal site, near Asufofuo in Sunyani. In the past, the site posed little or no threat because it was far away from human settlements, but today, urbanization and population growth have compelled people to develop lands surrounding the dump for new settlement. The threats the waste disposal site pose to the environment and the people who reside close to it provide the basis for planned remediation efforts to mitigate its impact on the environment.

Currently, the Sunyani Municipal Assembly (SMA) which manages the solid waste disposal site occasionally embark on certain remedial measures such as fumigation, compaction, spreading and covering methods as a way of mitigating the threats the site poses to the environment and public health. Fumigation, spreading and covering remedial measures by SMA only control mosquitoes and other vectors of various disease causing parasites at the dump while compaction, to some extent lowers the rate of leachate production but do not completely eliminate the potential dangers associated with the infiltration of leachate into the background geological materials and has the potential for groundwater pollution.

To make an effective assessment of the anthropogenic impact of solid waste in the environment and its potential for groundwater contamination, the entire volume of the waste and the geologic conditions of the site has to be comprehensively investigated. The most appropriate way of achieving this is by drilling numerous wells at close intervals in and around the waste disposal site to geochemically analyse collected core soil samples and leachate emanating from the site that infiltrate into the ground. However, these wells are expensive to drill. Also, any wells that are drilled and monitored are sparsely located because of monetary constraints (Shemang et al., 2011). Again, drilling alone provides localized information about the selected locations where samples were picked and may not therefore, give a true representative information about the overall possible pollution levels in the study area (Wemegah et al., 2014). On the other hand, non-invasive geophysical methods provide a better, fast and comparatively cost-effective means of acquiring information about the pollution levels in the immediate surroundings as well as the groundwater systems caused by solid waste disposals.

1.2 Statement of the research problem

The management of SWD sites is one of the major challenges that confronts local government authorities in most cities in Ghana. Metropolitan, Municipal and District Assemblies that have been charged with the responsibilities to manage solid and liquid wastes are noted for inefficient collection and disposal systems mainly due to financial constraints. As a result, most of the waste find their way into surface water bodies by run–off water from polluted sites whenever it rains. The collected wastes are usually transported and disposed off at unengineered waste disposal sites. These subsequently generate leachate that is produced when rainwater enters the refuse to combine with decomposed organic matter, rich in dissolved salts and containing enormous amount of pollutants (Porsani et al., 2004). The leachate naturally infiltrates into the groundwater to form plume that can compromise the quality of the underground water as indicated in figure 1.1 below.

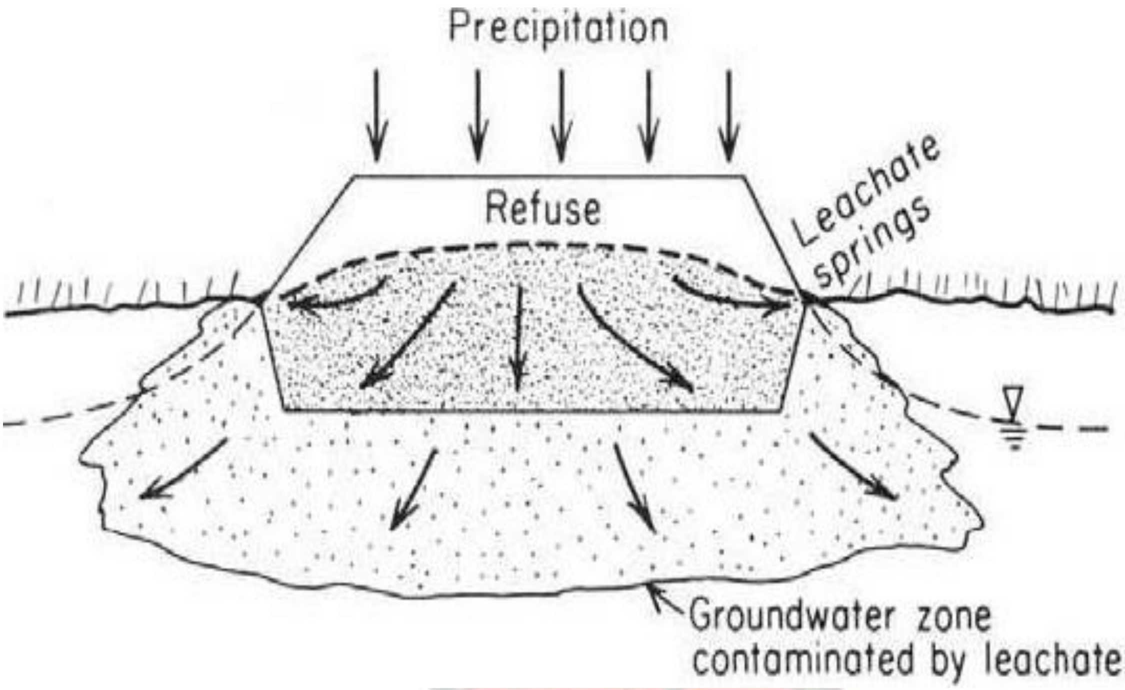

Figure 1.1: Conceptual diagram of leachate migration from a landfill and open dumps (World Health Organisation, 2006)

As the leachate percolates through the ground, many factors control the rate at which groundwater becomes contaminated. The depth to the water table is an obvious factor because the contaminants have to travel farther in deeper wells. Also, the stratigraphic layering, lithology and the underlying geologic formations among others have been ascribed as natural filters of some of the contaminants. The soil and the geological formations can slow down the migration of the contaminants or they may have the opposite effect depending on the porosity and permeability of the soil layers. For example, contaminants percolate more quickly through sandy formations than clayey formations. Similarly, the amount of precipitation at contaminated sites can accelerate the fluid flow rate through the ground.

The rain water that seeps into the ground can carry the contaminants dissolved in it into the aquifer to pollute it. Quite apart from these factors that control the rate of leachate migration through the soil, other forces and reactions that take place between the percolating leachate and the ground may result in alterations to the chemistry and a general reduction in the strength of the initial leachate amount. The forces and reactions may be biological in nature, chemical (hydrolysis, dissolution, oxidation and reduction reactions, adsorption, desorption, precipitation, and ion exchange) and physical (dispersion, absorption and filtration). Other established facts in literature indicate that certain factors can influence the rate of the leachate production. They include factors such as the composition of the waste, degree of compaction, moisture and temperature condition, particle size, age of landfill, available oxygen and the hydrology of the site (Jhamnani and Singh, 2009). Though, the soil filters, absorbs and removes many of the contaminants as they pass through the soil, it does not completely eliminate the potential for groundwater pollution (Boateng et al., 2013).

Previous geochemical analyses of leachate produced from landfills in different places indicated that the leachate percolating through the pore spaces from landfills into the groundwater systems was not safe for drinking at most locations (Abu-Rukah and Al-kofahi, 2001; Al-Yaqout and Hamoda, 2003). This is mainly as a result of the high chloride and sulphate ion concentrations with certain locations having high amount of heavy metals such as lead, cadmium, nickel, iron and zinc.

In cutting cost during remediation and at the same time lowering leachate production rate, it is indispensable for local authorities to acquire in-depth information about the subsurface geologic conditions and factors that control how groundwater becomes contaminated as discussed above and to identify zones of higher leachate activity using the appropriate geophysical techniques. In doing so, the much needed and exact remedial measures can be applied to mitigate the potential dangers unengineered landfills and open dumps pose to the natural environment.

1.3 Research objectives

The main objective for carrying out this research is to characterise the Sunyani municipal waste disposal site using integrated geophysical techniques.

1.3.1 Specific objectives

The specific objectives are;

- to detect and delineate possible zones of leachate contamination and accumulation in and around the solid waste disposal site.
- to detect and delineate possible leachate migration pathways around the site and to determine the vertical and lateral extent of incursions of leachate plume.
- to determine the thickness of the waste body.
- to delineate the physical boundaries and the area extent of the waste at the waste disposal site.

1.4 Justification for the study

The accelerated pace of urban population growth through migration from rural communities and changing lifestyles of the people, coupled with the increasing pace of economic and industrial development contribute large volumes of waste to the environment. The situation is further exacerbated when waste pollutes the already scarce downstream surface water and groundwater resources with potentially hazardous substances. The contaminants can be deleterious to public health and therefore, depth and area estimation of the solid waste, detection and delineation of contaminant plume from leachate generated at open dumps and waste disposal sites into aquifer systems has become a subject of interest to researchers and local authorities. The idea of determining the depth, boundary and the area extent of the waste is to estimate the volume of waste and the area of land space the waste covers since they can affect the amount of leachate that seeps into the ground.

Different scientific studies conducted on other sites relied mainly on geochemical analysis (Khanal, 2007; Denutsui et al., 2012) to evaluate the impact of the solid waste on the environment. However, these approaches have not yielded much in revealing the overall pollution levels in the entire catchment area of the dump. Hence the application of rapid and comparatively cost–effective integrated geophysical methods comprising of magnetic gradiometry, magnetic susceptibility and electrical resistivity tomography (ERT) to characterise the Sunyani municipal SWD site in order to acquire in–depth information about the thickness of the waste body, detection and delineation of possible plume contaminated zones that are potentially deleterious to public health.

It is therefore important that the dependence on groundwater in the vicinity of a waste disposal site by the surrounding households should be devoid of any potential pollution hazards that may expose them to serious health risks. The results of this study are expected to inform decisions on choosing a location for depositing waste, making provisions to underlie future waste disposal sites with protective liners made of clay or plastics, delineating boundaries around the waste disposal sites that are safe for drilling boreholes and ultimately to inform policy on municipal solid waste management and planning.

1.5 Project description and Scope of work

The research makes use of integrated geophysical methods comprising of ERT, magnetic gradiometry and magnetic susceptibility to characterise solid waste disposal site by determining the presence of plume, delineating pathways leachate migration as well as determing the geometry (thickness and lateral extent) of the waste in Sunyani municipality. The data collected would be processed using geosoft, grapher, arcgis and res2dinv softwares to make meaningful interpretation from the data.

1.6 Literature Review

SWD sites are potential sources of environmental pollution and poor management of the sites can lead to hazardous implications for the environment and public health. Among the health implications occasioned by the lack of effective and efficient waste management system include frequent outbreak of epidermic and communicable diseases directly conveyed by vectors which serve as agents for many disease causing parasites. Indirectly, the health implications may result from the release of leachate that may infiltrate into the ground to render groundwater unsafe for drinking and other domestic purposes. Also, seepages of leachate into groundwater resources may present a real danger to aquatic lives if the contaminated groundwater from the leachate plume discharges into nearby streams through a eutrophication process. It is also worth noting that SWD sites impact on the environment negatively as they disrupt scenic landscapes, introduce unpleasant smells and greenhouse gases that contribute to global warming.

In this research, i seek to bring to the attention of city authorities, the consequences of MSW landfilling in order to influence decision on legislation about developments around the waste disposal site. At present, no detailed scientific investigation has been carried out at the site. A cursory look at other studies conducted elsewhere made use of chemical and physico–chemical analyses. Al-Yaqout and Hamoda (2003) investigated two different unlined MSW disposal sites, of differing ages in Kuwait in order to chemically characterise leachate and examine the leachate formation mechanisms. In their work, data on Leachate quality were collected from the two sites where co-disposal of MSW and the other, solid and liquid wastes is practised. The analysis of the acquired data confirmed that leachates emanating from the two waste disposal sites are extremely contaminated with heavy metals, organic compounds and salts.

Abd El–Salam and Abu-Zuid (2015) also applied physico–chemical analyses to investigate the environmental impacts of SW landfilling, by analysing the quality of leachate and groundwater near various landfill sites in Egypt. The results of the physico–chemical analyses confirmed that leachate characteristics were highly variable with extreme contamination of heavy metals, salts and organic compounds. The BOD_5/COD ratio of 0.69 obtained from their results indicated that the leachate was biodegradable and un–stabilized. It was also discovered that groundwater in the vicinity of the landfills did not have severe contamination, even though certain parameters exceeded the WHO and EPA limits.

In addition to the above methods, several other geophysical techniques have also been used in previous studies to map the spatial distribution of physical properties to which each method is sensitive at various waste disposal sites. Using the physical properties, these geophysical methods have helped in delineating the boundaries, determining the internal structure and the composition of the waste deposit as well as mapping contaminated zones around waste disposal sites. Among the methods are electromagnetics (EM)(Boateng et al., 2013), magnetics (Wemegah et al., 2014; Marchetti et al., 2002), electrical resistivity (ER) (Fadhli et al., 2015), ground penetrating radar (GPR) (Shemang et al., 2011), induce polarization (IP) (Gazoty et al., 2012) and recently, gravity (Mantlik et al., 2009). ER, IP, EM, GPR and magnetic geophysical techniques can be employed to investigate landfills because leachate can greatly influence the Earth's physical properties such as resistivity and or conductivity, chargeability, magnetic susceptibility and dielectric constant (Abdullahi et al., 2011). Other factors that include concentration of plume in the ground, the nature of background soil or bedrock, type of delineation (i.e lateral and vertical or both), depth of investigation and type of plume can also influence the choice of each method.

Exploration of subsurface minerals, geological structures and other information are carried out using different geophysical exploration techniques to complement each other in order to remove some of the ambiguities associated with just a single method. Therefore, the integration of different geophysical methods enables scientists to better characterise and map the physical properties of various waste disposal sites, their subsurface and their close surroundings (Belghazal et al., 2013). In many environmental applications such as monitoring of seepage zones and delineation of landfill sites or monitoring of leakages from underground storage tanks (UST), electrical resistivity imaging (ERI) has been used to identify fluid migration and pathways in the subsurface. Due to the fact that fluids have varying electrical resistances, the ERI has become nearly an ideal tool for imaging fluid electrical signatures to determine the fluid flow patterns. Similarly, magnetic surveys as a traditional mapping tool has proved to be very effective for detecting sporadically distributed magnetic signatures derived from buried metals in waste.

In literature, many researchers around the world have successfully applied multiple geophysical methods to solve many problems in mineral exploration, civil engineering, hydrogeological studies and environmental applications (Gilkeson et al., 1992; Marchetti et al., 2002; Cochran and Dalton, 1995; Bernstone and Dahlin, 1997; Shemang et al., 2011; Wemegah et al., 2014) among others.

DC electrical resistivity method has been applied in various fields to map the lateral and vertical discontinuities in subsurface resistivity. The resistivity of the subsurface decreases with increasing concentration dissolved salts, organics and heavy metals thereby making the DC electrical resistivity method the most preferred choice for detecting and mapping leachate plumes. A plume is an underground pattern of contaminant concentrations created by the movement of groundwater beneath a contaminant source (Boateng et al., 2013) with its migrating edges called plume fronts. The contaminant plume follows the hydraulic gradient of the study area as it spreads mostly, laterally in the direction of the groundwater flow. The sources of original contamination mostly have the highest concentration of contaminants and its magnitude decreases as it moves farther away from the contaminant source. Due to the high concentration of chloride, fluoride ions and other heavy metals, ground contamination from waste disposal sites are more electrically conductive than the surrounding formation that contains small amount of contaminated pore water. For this reason, it has become possible to use plumes and plume fronts containing these ions to locate the source of contamination, detect water pollution and to map the lateral extent of incursion within an aquifer using the electrical resistivity method.

Lemke and Young (1998) describes mise-`a-la-masse (MALM) electrical resistivity method in their investigations to trace contaminant plumes from landfills in Michigan. Similar work has been done using electrical resistivity tomography (ERT) and MALM to ascertain leachate confinement in sanitary landfills by the high-density poli-ethylene (HDPE) liner (De Carlo et al., 2013). Others have also applied it to monitor contaminated sites by delineating the contamination extent of migration from a polluted source. The ERI has also been successfully applied to detect and map karst geomorphology and groundwater migration patterns (Fadhli et al., 2015; Vouillamoz et al., 2003; Van Schoor, 2002).

Resistivity surveys for mapping and characterising SWD sites are particularly effective in areas that have sufficiently large contrast in resistivity between the landfill and the surrounding undisturbed material. However, in areas where the resistivity of the surrounding background material is significantly low, typical landfills may have similar resistivity compared to the background geologic materials, and therefore difficult discriminating it from the surrounding geology. Also, because of the fundamental limitation that resistivity varies strongly with variations in moisture content which can mask local resistivity changes due to the waste, electrical resistivity surveys alone are not sufficient mapping tool for delineating landfills. As a result, time-domain induced polarization (IP) surveys together with ER surveys (Carlson et al., 2001; Dahlin et al., 2010; Dahlin, 2012) and magnetics (Wemegah et al., 2014) in recent times have become very popular in buried landfill mapping. In most environmental applications, IP techniques have been successfully applied to map out areas where conductive materials are concentrated. Also, IP surveys have been used to detect and delineate non-metallic areas in landfills that are transparent to magnetic surveys (Carlson et al., 2001). It is mostly carried out by measuring the chargeability of the waste composite and its close surroundings since the waste produces strong IP signatures as a result of high concentrations of ions percolating through the ground.

Similarly, the magnetic method as a traditional mapping tool has proved to be very effective for solving environmental problems by detecting local perturbations in the Earth's magnetic field strength called magnetic anomalies (e.g., Wemegah et al., 2014; Shemang et al., 2011; Marchetti et al., 2002; Furness, 2007; Marchetti and Settimi, 2011) in recent times. This is based on the fact that the magnetic response of rocks, ferromagnetic materials and other heavy metals such as iron, nickel, cobalt etc., in municipal waste composite is determined by the amount of mineral constituents, the distance from the sensor and their magnetic susceptibilities. Invariably, metallic objects composed of heavy metals, steel and other ferromagnetic materials at shallow depths have significant magnetic anomalies.

Every material has an inherent physical property called magnetic susceptibility, which is a measure of the ability of the material to become magnetised under the influence of an external magnetic field. In topsoil studies, the type of magnetic minerals and the amount present in soil as well as rock samples greatly influence the susceptibility values. These magnetic minerals may either be of lithogenic origin, derived from a parent rock during pedogenisis or as a result of anthropogenic activities. Le Borgne (1955) first reported of soil susceptibility enhancement and has been confirmed by other researchers worldwide (e.g., Mullins, 1977; Thompson and Oldfield, 1986; Singer et al., 1996). Several studies have also revealed close correlation between soil magnetic susceptibility and heavy metal content in topsoil investigations (e.g., Schmidt et al., 2005; Karimi et al., 2011; Strzyszcz and Magiera, 1998; Petrovsky et al., 2000). As a result, the magnetic susceptibility method as proxy for the geochemical method in recent times has become very popular in topsoil investigations of heavy metal content because contaminants and magnetic minerals are genetically related (Hanesch and Scholger, 2002). More importantly, data acquisition is fast and less laborious on large terrains. Therefore, when used together, the gradiometric and magnetic susceptibility data sets could be used to map and discriminate ferrous from non-ferrous metallic waste in unsorted pre-to-disposal municipal solid waste sites (Wemegah et al., 2014) as well as acquiring information about the lateral extent of the waste deposit.

Wemegah et al. (2014) reported having used integrated geophysical methods comprising of magnetics, DC electrical resistivity and time-domain induced polarization to characterise Ohwim waste disposal site in the Kumasi Metropolis. They explained that environmental pollution from solid waste landfilling poses serious risk to groundwater and downstream surface water resources, especially when landfilling is carried out without any protective layer underneath the waste deposits. From their results, zones of likely pollution plumes were identified. Also, while the result from the magnetic survey showed the strength of the magnetic data in mapping the lateral extent of the waste deposit, DC electric resistivity and the full wave induced polarization tomography on the other hand mapped the vertical extent of the dumpsite and characterised the hosting geology.

The effective application of magnetometric surveys in various waste disposal sites has been reported by Marchetti et al. (2002); Marchetti and Settimi (2011) to detect buried steel drums. A preliminary magnetometric survey conducted by (Marchetti et al., 2002) revealed the existence of anomalous zones in a tuff quarry in Riano Flaminio (north Rome, Italy). In order to confirm that the anomalous zones were generated by underground magnetic materials, excavations were carried out over the causative bodies. In all, 160 steel drums were found. After removing them, a new magnetometric survey was conducted on the same area. To better characterise the subsoil, a multi–frequency induction survey, a geoelectrical and GPR surveys were conducted on the basis of the new magnetic anomaly map.

Marchetti and Settimi (2011) tested the effectiveness of integrated geophysical methods comprising of a magnetometric survey, DC electrical resistivity tomography with different arrays and a multi–frequency frequency-domain electromagnetic survey in clayey–sandy ground where twelve (12) empty steel drums had previously been buried at 4–5 m below ground level. The results of their study clearly indicated that both the magnetometric and electromagnetic induction surveys actually detected the steel drums that had been buried in the subsurface, while the electrical resistivity tomography mainly detected some physical property variations of the terrain connected with the digging operations, instead of detecting the actual presence of the steel drums.

Indeed, the numerous successes attained with the effective application of some geophysical methods in monitoring pollution levels at contaminated sites cannot be underestimated. In recent times, they have gained a lot of popularity because of the comparative advantage they have over the other surrogate methods (i.e chemical and physico–chemical analyses). Based on the age of the SWD site which spans over twenty–three years and the successes reported in this work with the methods mentioned above, it is expected that the integration of ERT, magnetic susceptibility and magnetic gradiometry methods will achieve the stated objectives.

1.7 Structure of Thesis

Chapter one gives an introduction to the work, an overview of the field of geophysics, its advantages and limitations, the objectives of the study, justification of the research topic and finally, the general literature review of the research topic and related research works in the past. Chapter two generally reviews SW and the various ways of classifying the waste. It also reviews the amount of waste generated in some selected cites in Ghana. It again throws more light on the collection, transfer, disposal of MSW and existing waste management policies. Chapter three outlines the theoretical background and the physical principles of the various methods applied to the study. Chapter four looks at the study area, its location, climate and vegetation, economic activities of the inhabitants and the local geology. It also provides an overview of the research methodology, the instrumentation and materials used to address the specific objectives. Chapter five discusses the results obtained from the gradiometric, magnetic susceptibility and electrical resistivity surveys for some profiles. Chapter six draws a conclusion from the research work based on information derived from the various geophysical surveying methods to fit the objectives of the research. It also includes suggested recommendations about the use of other methods to support the results obtained in this work.

Chapter 2

MUNICIPAL SOLID WASTE MANAGEMENT

2.1 Municipal Solid Waste

Municipal solid waste refers to the undesired remains, discarded materials or by-products which are no longer required for the initial use and may consist of such items like papers, woods, plastics, metals, glasses, textiles, organic materials, etc., generated from households, commercial centres and institutions (Osei-Mensah et al., 2014). Studies by other researchers have shown that most of the municipal solid waste that are generated from developing countries come from households (55–80%), with commercial centres contributing (10–30%) and the smallest proportions coming from institutions (Nagabooshnam, 2011) such as school, banks, government agencies etc.. According to (Miezah et al., 2015), the organic fraction of the waste composite was highest in the waste stream and accounts for about half the total waste collected.

2.2 Global Waste Management Outlook

Municipal solid waste management (MSWM) system basically deals with the direct generation, source separation, storage, collection, transport, processing, treatment, recovery and disposal of solid waste that conforms to best principles of public health, engineering, conservation and other environmental considerations. This system is popularly practised in developed countries in Europe, the Americas and Asia that have standardised waste management systems, well defined policies and enforceable legislations.

Waste production and generation have seen a tremendous increase as much as ten folds in the last century because the world's population has enormously soared and become more urban and affluent. The world's population of urban residents in 1900 was about 220 million which accounted for about 13% of the total world's population. They produced lower than 300,000 tonnes of MSW per day. By the end of 2000, a total of 2.9 billion urban residents accounting for about 49% of the world's population were generating over 3 million tonnes of solid waste per day (Hoornweg et al., 2013). It is projected that the world's total SW generation would double by 2025 and this is expected to be driven by forces like, rural–urban migration, population growth, changing lifestyles, rising waste per capita as economies grow among others. It is apparent that these driving forces are interconnected and any variation in one automatically affects the other. In Ghana, Miezah et al. (2015) reported that the affluent produced the most waste in the society and on a global scale, a survey conducted by the United Nations Environment Programme UNEP (2015) in some selected countries also revealed that MSW per capita increases with gross national income (GNI) of the selected countries as shown in figure 2.1

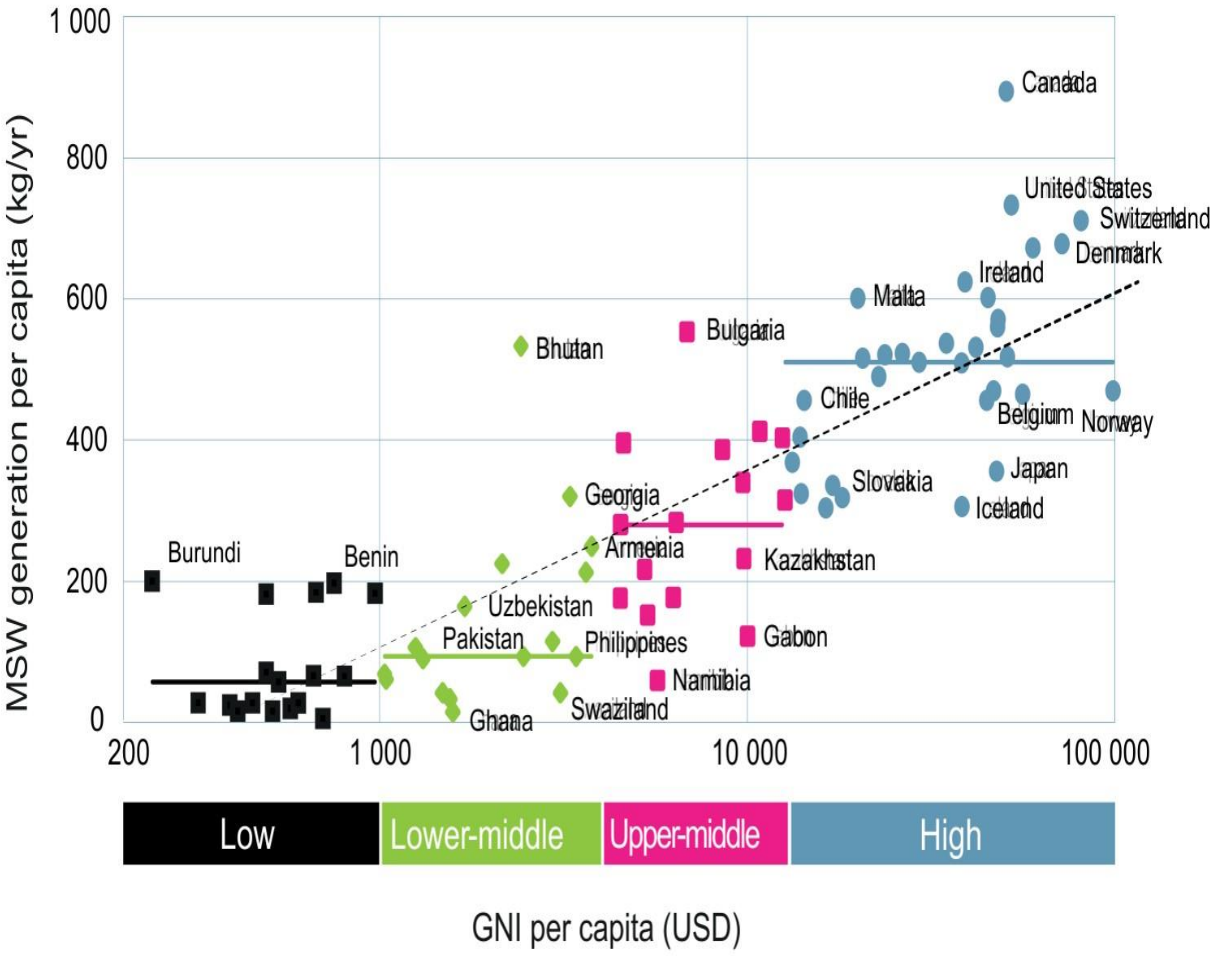

Figure 2.1: MSW Per Capita Increases with Income Level for Selected Countries (Modified from UNEP (2015)

SWM is among one of the major areas that drains municipal budgets. According to the World Bank (2013), the cost of dealing with all the generated waste globally is also on the rise: from $205 billion a year in 2010 to $375 billion by 2025, with the sharpest cost increases in developing countries. The increasing financial budget for managing the waste makes it difficult for local authorities to execute their mandate effectively and as a result, a considerable percentage of the waste in developing countries as well as lower–middle income countries remain uncollected. Notably, the little quantity of waste collected is also predominantly characterised by poor management practises (i.e. collection, haulage and landfilling). On the contrary, high income earning countries have greater waste collection coverage as indicated in figure 2.2 below.

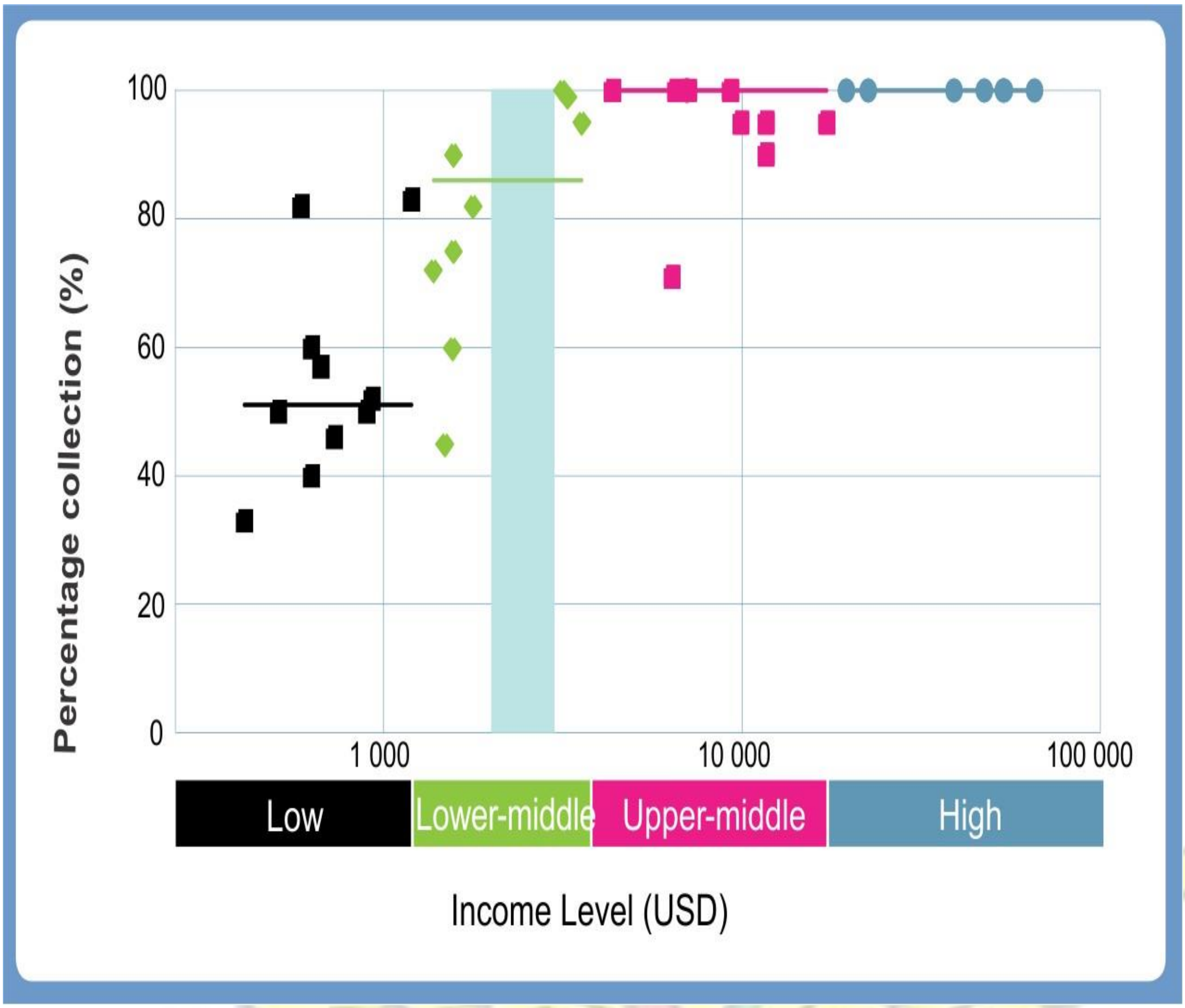

Figure 2.2: Waste Collection Coverage for Selected Countries (Modified from UNEP (2015)

2.3 Waste Management Policies in Ghana

In the face of the numerous benefits that one can derive from modern waste management practices, the system in Ghana is overwhelmed with various challenges of different magnitudes that greatly affect the effectiveness and smooth operations of service providers. These challenges include inadequate waste management inputs, absence of enforceable regulations on environmental sanitation, lack of technical expertise and logistical constraints, poor perception and attitude of people towards waste and environmental sanitation, lack of awareness, improper collection, segregation, transportation and disposal methods, lack of community involvement and above all insufficient funds.

The management of waste in Ghana generally is the responsibility of the Ministry of Local Government and Rural Development (MLGRD), which plays supervisory role over all the decentralized Metropolitan, Municipal and District Assemblies (MMDAs). However, the Environmental Protection Agency (EPA) under the auspices of the Ministry of Environment, Science, Technology and Innovation is vested with the regulatory authority to develop the appropriate operational framework. The MMDAs have the responsibility of collecting, hauling and finally disposing off the solid waste through their Waste Management Departments (WMDs) and their Environmental Health and Sanitation Departments.

The National Environmental Sanitation Policy Coordinating Council (NESPoCC) has been established to expedite action on the implementation of the National Sanitation Policy. Generally, the NESPoCC has the responsibility of coordinating the policy and ensuring effective communication and cooperation between the key actors and allied agencies involved in environmental management in the Districts. The laws comprising the Criminal Code (Act 29), 1960 and the Bye-laws of the various MMDAs are sufficient to support the efficient delivery of environmental sanitation services and ensure compliance of regulations. However, it is apparent that our current predicament is a manifestation that authorities are not enforcing strict compliance with the sanitation rules due to logistical problems and financial constraints. These make the MMDAs handicapped in ensuring clean, safe and healthy environment.

In order to address the numerous problems that engulf the waste management service delivery, there has been a major shift in the waste management practices as spelled out in the revised Environmental Sanitation Policy ESP (2010). According to the policy, the collection and sanitary disposal of wastes shall be the responsibility of the WMDs within Metropolitan and Municipal Assemblies or District Environmental Health and Management Departments of District Assemblies (DEHMD). These services can be provided either directly or indirectly through private contractors or franchisees. The implementation of the ESP (2010) with the cost recovery component has shifted the huge financial burden from the Assemblies to the citizenry through the polluter–pays principle. Despite this new development, the policy mandates the Assemblies to maintain an in-house capacity to provide at least 20% of the sanitary services directly. The WMDs of the various assemblies now, practically perform supervisory functions over private waste management companies as far as the management of SW is concerned. Prior to the revision, the ESP (1999) sought to strengthen the various key and allied institutions as well as coordinate their activities to achieve a common goal. The policy strategy outlined are;

- Formal establishment of environmental sanitation as a sub-sector within the national development programme.

- Rationalization of institutional objectives and functions at all levels, including delegation of responsibilities and the establishment of inter–agency linkages.

- Establishment of the NESPoCC within the MLGRD.

- Establishment of a National Environmental Sanitation Day to be observed one day in a year by all citizens.

- Development and strengthening of the communitys role in environmental sanitation.
- Development of human resources and strengthening institutional structures for managing environmental sanitation.

- Assigning delivery of a major proportion of environmental sanitation services to the private sector through contract, franchise, concession and other arrangements.
- Development of a strong legislative and regulatory framework, and capacity for supervising environmental sanitation activities and enforcing standards.
- Promotion of research to review sanitation technologies.
- Identification and dissemination of cost-effective, appropriate, affordable and environmentally friendly technologies to address environmental sanitation needs.
- Adoption of the cost recovery principle in the planning and management of environmental sanitation services.

2.4 Waste Management Practice in Sunyani

Current solid waste management practice (i.e., collection, haulage and landfilling) at the SMA waste disposal site has direct implications on the environment. They include the generation and emission of greenhouse gases like methane which contribute to global warming, unpleasant smells, destruction of scenic landscapes and issues of land management. A cursory look at contemporary and proper waste management practices in some developed nations points to the integration of waste reduction, source separation, reuse, recycling and treatment, composting and waste-to-energy in order to minimise the daunting challenges the current system poses to the environment. Undoubtedly, it is apparent that such waste management practices are more sustainable, environmentally acceptable and economically prudent.

The management of solid waste over the years has been an albatross around the neck of city authorities in Ghana. The Sunyani Municipal Assembly (SMA) and private waste management firms still continue to grapple with the collection of the large volumes of solid waste generated daily. Undoubtedly, the capacity of city authorities has been overwhelmed by the ever-increasing volumes of waste at urban centres due to population growth. Like other cities in Ghana, waste management in Sunyani falls under the Ministry of Local Government and Rural Development, which presides over the 216 Metropolitan, Municipal and District Assemblies (MMDAs). The SMA was responsible for the collection, haulage and final disposal of solid waste until recently, when the Government of Ghana in order to ensure greater efficiency in waste management decided to embrace the idea of private participation into the sector through the environmental sanitation policy promulgated in 1999. In this regard, the primary function of collection, haulage and disposal of the solid waste by SMA has been contracted to Zoomlion Ghana Limited; a private waste management firm.

2.4.1 Waste Generation and Collection

MSW generated from domestic, commercial centres and institutions comprises of highly heterogeneous mass of unwanted materials that have variable physical characteristics depending on their sources. The waste can be classified into two groups, organic and inorganic. The organic waste mainly consists of papers and cardboards, food waste, wood, garden waste just to mention few. The inorganic waste is made up of cans, glass, electronic waste, bottles, metals, plastic, etc.. According to Miezah et al. (2015), the geographical location, income level of an area, economic activity and occupation could also influence waste generation. In Sunyani municipality, Miezah et al. (2015) reported that high class income areas have the highest per capita generation rate of 0.52 *kg* per day, followed by middle class income areas with 0.49 *kg* per day and subsequently 0.47 *kg* per day for low class income areas. The estimated waste generation rate for the municipality is pegged at 110,976 *kg* per day. Table 2.1 shows the waste generation rate projections based on 2010 figures.

Year	2012	2013	2014	2015	2016
Pop. Growth Rate(%)	3.8	3.8	3.8	3.8	3.8
Total Population	209,035	216,979	225,220	233,783	242,667
Per Capita Gen.(Kg/d)	0.45	0.45	0.45	0.45	0.45
Total Gen.(t/d)	94.07	97.64	101.35	105.20	109.20
Total Gen.(t/a)	34,334.09	35,633.60	36,992.75	38,398.00	39,858.00
Total Gen.(m^3/d)	266.21	276.32	286.82	297.73	309.04
Total Gen.(m^3/a)	97,166.63	100,856.80	104,689.30	108,671.45	112,799.6

Table 2.1: Waste Generation Projections for Sunyani (Owusu, 2010)

There are two main types of SW collection services provided by private companies in Sunyani. The door-to-door services which is patronised by high income and some middle income class areas and the communal container collection services by the low income class areas. With the door-to-door collection, the individuals living in apartments, well laid-out housing systems and other high income earners and institutions store their wastes in waste bins that have been provided by the private waste management company. The private waste management companies collect household wastes using waste *Compactors*, *Skip* vehicles and sometimes *tricycles* for their door-to-door collection services at a fee. For the communal collection services, individuals predominantly use polyethylene plastic bags and woven baskets for collecting waste generated in their various households. The waste is sent to the communal container sites at designated locations in the communities. Contrary to what pertains elsewhere in other cities in Ghana (i.e, Accra and Kumasi), the communal collection services is free of charge in order to discourage indiscriminate disposal of waste in poor communities in Sunyani municipality. The collected waste is then picked up and hauled to the landfill site by the private companies. The different types of waste generally are not separated at source but are mixed up by the individuals and then disposed in the waste containers.

2.4.2 Municipal Solid Waste Transportation

The waste collected by Zoomlion Ghana Limited (*ZL*) at the various common collection points (public dump containers) and those collected through its door-to-door services are then transported and disposed off in the SMA waste disposal site without any pre-treatment, as there is no existing recycling facility in the municipality. The haulage of the waste is done by means of *Compactors* and *Skip* vehicles or sometimes *Tricycles*.

2.4.3 Final Disposal

Landfilling offers the cheapest alternative to city authorities for the disposal of MSW as it is still the main method of waste management employed by the municipal assembly and *ZL*. The waste dumped in the waste disposal site is spread, compacted and covered with soil using a bulldozer. Prior to that, recovery activities by scavengers take place at the site. The recyclable materials like cans, scrap metals, plastics etc., that are recovered from the waste disposal site are transported to Accra to be recycled and reused. Scavenging plays an important role in reducing the volume of waste in the waste disposal site whiles serving as a source of livelihood for many people. According to Moreno-Sanchez and Maldonado (2006), the informal waste-pickers in developing countries collect about 40% of recyclable material mostly, plastics and metals from the waste stream.

2.5 The SMA Waste Disposal Site

The SMA waste disposal site near Asufofuo was constructed by the Assembly and commissioned in the early nineties with an expected life span of 35 years. It is unlined and offers the easiest and cheapest means of SW management for city authorities. It is about 2.5 *km* from the city centre and covers a land size of about 0.2 km^2. The station is managed by environmental health office at the WMD of the SMA. The site is equipped with a bulldozer for spreading and compacting the waste dumped at the site.

Figure 2.3: The SMA Waste Disposal Site near Asufofuo

Chapter 3

THEORY OF GEOPHYSICAL METHODS USED

3.1 Electrical Resistivity

Electrical resistivity is a fundamental material property which is a measure of the ability of the material to oppose the flow of current flowing through it. In the field of geophysics, the purpose of electrical surveys is to determine the subsurface resistivity distribution by making direct measurements on the ground surface in order to locate local features of interest. In measuring the resistivity of a cross-section of the Earth, current is injected into the ground through a pair of current electrodes and the response (voltage) is measured across the second pair of potential electrodes. In a homogeneous ground, the current flows radially away from the electrode and it is distributed uniformly over a hemispherical shell centred on the source (Kearey et al., 2002). As current paths cross an interface separating different resistivities, they refract much as seismic waves encountering an interface. However, unlike the case of seismic waves, current paths refract towards the normal when crossing into rock with higher resistivity, and away from the normal in rock with lower resistivity (figure 3.1). Electric current can be conducted through rock matrices in three main ways. These are:

- *electrolytic conduction* which is the conduction of electrical current by the relatively slow movement of ions through the pore fluids in rocks.
- *electronic conduction* is the process by which electrically charged particles (electrons) move rapidly through metals in response to an applied electric field.
- *dielectric conduction* occurs in rocks and minerals with high resistivity when an external alternating current is applied.

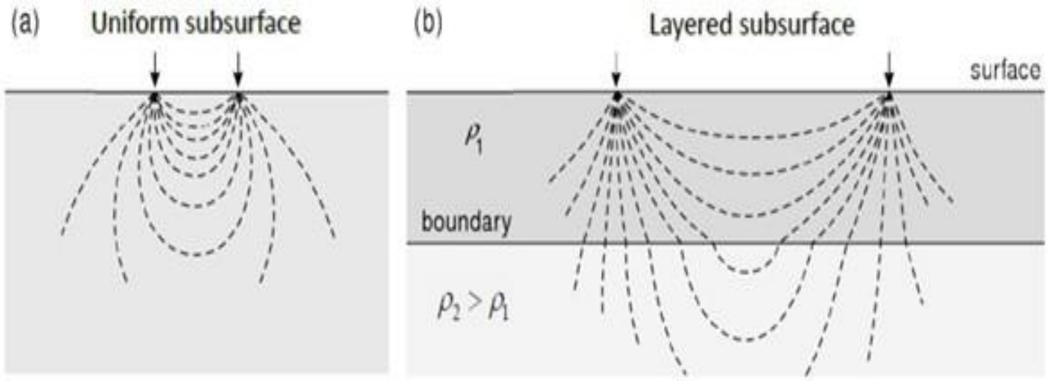

Figure 3.1: Qualitative Distribution of Current Flow Lines. (a) Homogenous Subsurface (b) Layered Subsurface. (Modified from Palacky (1988))

In rocks and soils, current flows primarily by electrolytic conduction with the pore fluids acting as electrolytes. The actual mineral grains and solid rock matrices contributes very little to the flow of current because they are semi-conducting, with few exceptions that are metallic and other surfaces of some clay minerals. The ground resistivity varies because it is controlled by geological parameters such as mineral and fluid content in pore spaces, porosity and degree of compaction among others. For example, sedimentary rocks have low resistivity signatures due to the high content of fluids contained in their pore spaces, while igneous rocks tend to have the highest resistivity values. In view of the above, there is a clear overlap between the resistivities of the different rock types and that makes it impossible to identify the different rock types solely on the basis of resistivity data as shown in figure 3.2.

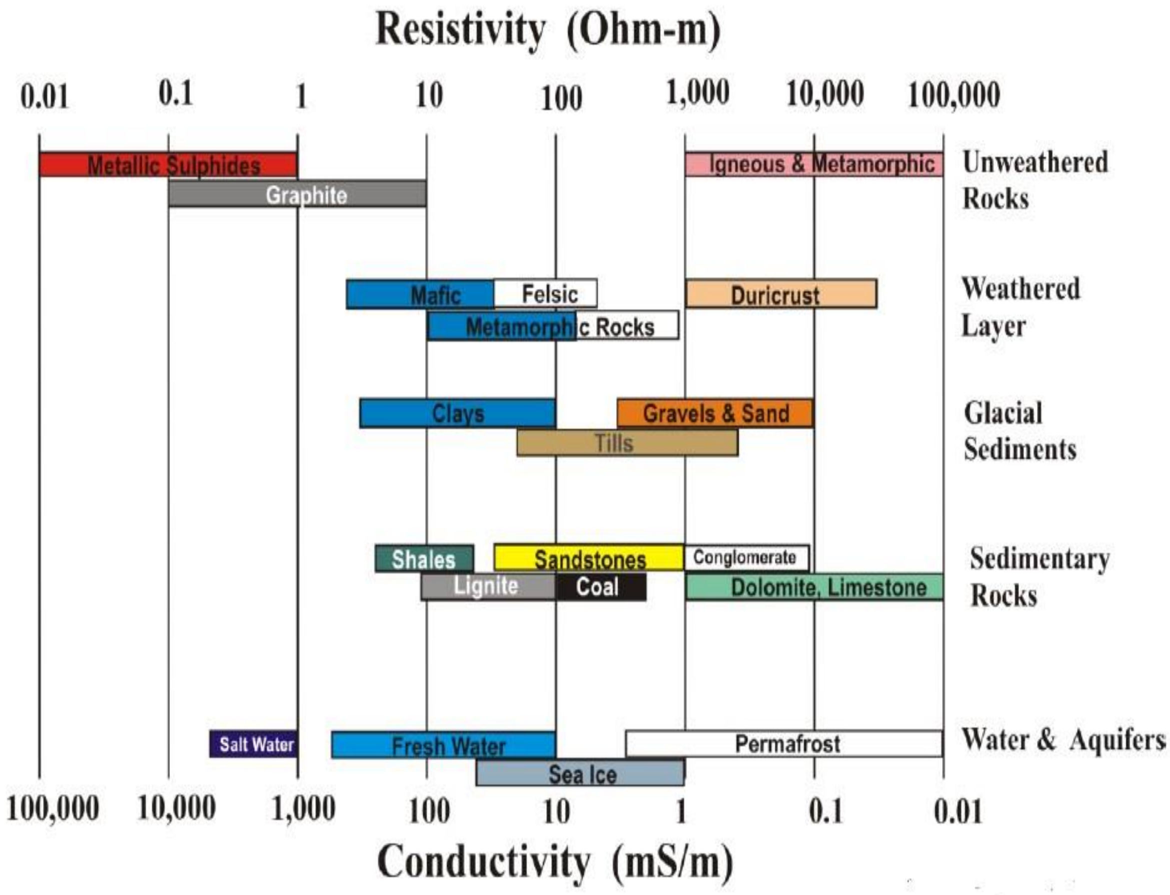

Figure 3.2: Electrical Resistivity of Rocks, Minerals and Soils (Modified from Palacky (1988))

3.1.1 Basic Theory of Electrical Resistivity Method

The resistivity measurements are normally made by injecting current into the ground through two current electrodes, (a source A and a sink B), and measuring the resulting potential difference at two potential electrodes M and N. The current flow paths and surfaces of constant voltage called, equipotential surfaces are shown in figure 3.3. According to Kearey et al. (2002), the potential V_M at point M is due to the potential contributions of V_A and V_B from the current at source A and sink B;

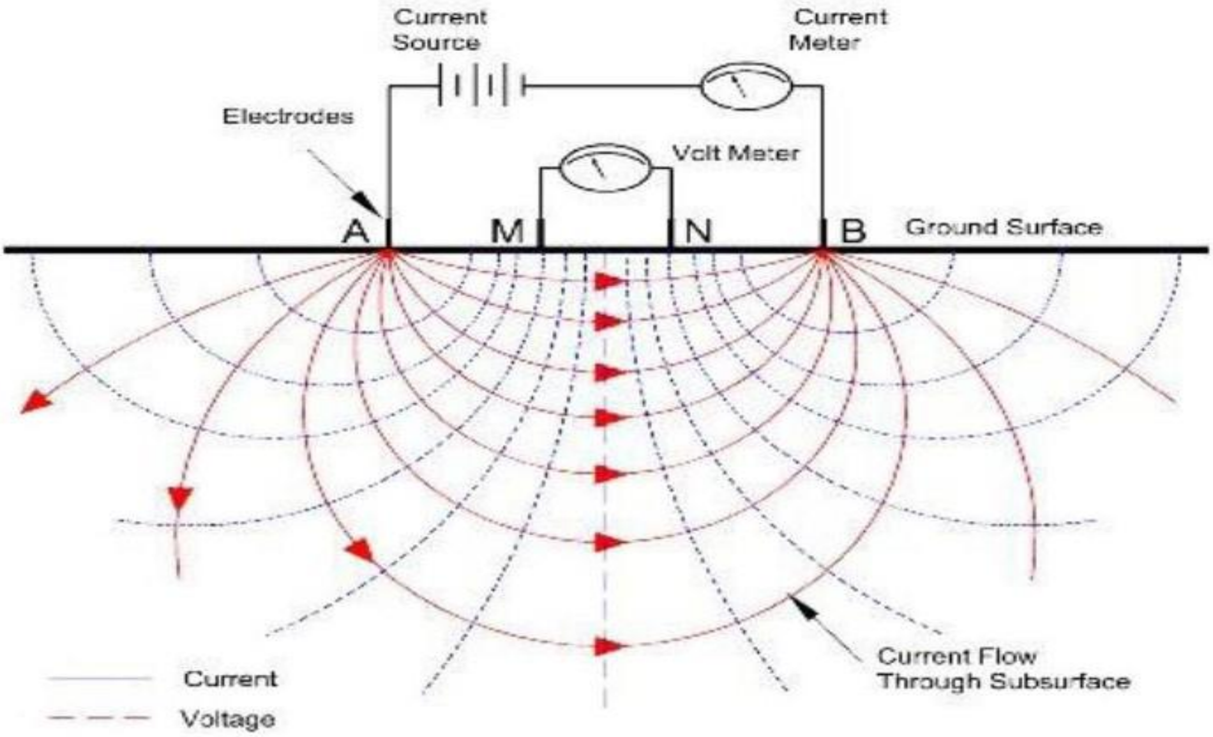

Figure 3.3: Current Patterns and Equipotential Surfaces in a Homogeneous Ground

Thus $V_M = V_A + V_B$, where $V = \frac{I_i \rho_a}{2\pi r}$

$$V_M = \frac{I_i \rho_a}{2\pi}\left[\frac{1}{|AM|} - \frac{1}{|MB|}\right] \tag{3.1}$$

where $|AM|$ and $|MB|$ are the distances from the current electrodes to the potential electrode at point M. Similarly, the potential V_N at N is given by:

$$V_N = \frac{I_i \rho_a}{2\pi}\left[\frac{1}{|AN|} - \frac{1}{|NB|}\right] \tag{3.2}$$

Where $|AN|$ and $|NB|$ are the distances from the current electrodes to the potential electrodes at point N. The potential difference ΔV between the electrodes, M and N is given by:

$$\Delta V = (V_M - V_N) = \frac{I_i \rho_a}{2\pi}\left[\frac{1}{|AM|} - \frac{1}{|MB|} - \frac{1}{|AN|} + \frac{1}{|NB|}\right] \tag{3.3}$$

This simplifies to

$$\rho_a = \frac{2\pi\Delta V}{I_i}\left[\frac{1}{|AM|} - \frac{1}{|MB|} - \frac{1}{|AN|} + \frac{1}{|NB|}\right]^{-1} \tag{3.4}$$

$$\rho_a = \frac{k\Delta V}{I_i} \tag{3.5}$$

where

$$k = 2\pi\left[\frac{1}{|AM|} - \frac{1}{|MB|} - \frac{1}{|AN|} + \frac{1}{|NB|}\right]^{-1} \tag{3.6}$$

where ρ_a is the apparent resistivity and k is the geometric factor that describes the geometry of the electrode configuration being used and also the arrangement of the four electrodes. The resistivity meter normally gives a resistance value, $R = V/I_i$, so in practice the apparent resistivity value is calculated by $\rho_a = kR$. The calculated resistivity value is not the true resistivity of the subsurface, but the apparent value which is the resistivity of a homogeneous ground that will give the same resistance value for the same electrode arrangement. The relationship between the apparent resistivity and the true resistivity is a complex one. In order to obtain a true resistivity information about the subsurface, an inversion of the measured apparent resistivity values using a computer program is carried out.

3.1.2 Electrode Configuration

There are several electrode configurations or arrays that have been designed to suite various specific objectives and applications. These may include depth sounding and lateral profiling or a combination of both as well as the subsurface resolution. These arrays include the wenner, schlumberger, dipole–dipole, pole–pole etc.. The arrays are discussed below.

3.1.2.1 Wenner Array

The Wenner array is one of the most widely used electrode configuration because of its numerous capabilities. It is sensitive to vertical changes in the subsurface resistivity below the centre of the array. However, it is less sensitive to horizontal changes. In general the Wenner is good in resolving vertical changes (i.e horizontal structures), but relatively poor in detecting horizontal changes (i.e narrow vertical structures) (Loke, 2000). The median depth of investigation is approximately half the electrode spacing used for a single profile line. Compared to other arrays, the Wenner array has a moderate depth of investigation and has the strongest signal strength which makes it an important factor to consider if the survey is to be carried out in areas of high background noise (Loke, 2000).

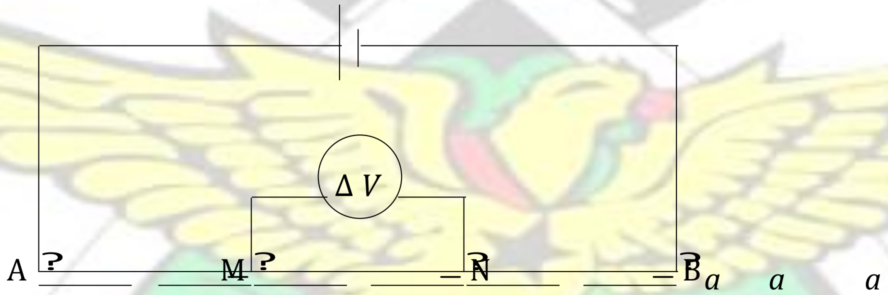

Figure 3.4: Wenner array (Modified from Kearey et al., 2002)

For this array, both the current and potential electrodes are maintained at an equal spacing (a) as in figure 3.4. From this figure, $|AM| = a$; $|MB| = 2a$; $|AN| = 2a$ and $|NB| = a$.

Substitution of these conditions into equation 3.3 yields

$$\Delta V = \frac{I_i \rho_a}{2\pi}\left[\frac{1}{a} - \frac{1}{2a} - \frac{1}{2a} + \frac{1}{a}\right] \tag{3.7}$$

$$\Delta V = \frac{I_i \rho_a}{2\pi a} \tag{3.8}$$

$$\rho_a = \frac{2\pi a \Delta V}{I_i} \tag{3.9}$$

$$\rho_a = 2\pi a R \tag{3.10}$$

Hence, for the wenner array, $k = 2\pi a$

3.1.2.2 Schlumberger array (asymmetrical)

The Schlumberger array (asymmetrical) also referred to as the Gradient array has the potential electrodes within the current electrodes which are at the extreme ends of the four electrode system. In taking measurements, the potential pair is moved between the current pair. Gradient array is one of the most commonly used array for resistivity profiling due to the relative ease of the deployment and the fact that only two electrodes are moved between successive readings. From figure 3.5,

$|AM| = (L - x) - l$, $|MB| = (L + x) + l$, $|AN| = (L - x) + l$ and $|NB| = (L + x) - l$

Substituting the above into equation 3.4 gives

$$\rho_a = \frac{2\pi\Delta V}{I_i}\left[\frac{1}{(L-x)-l} - \frac{1}{(L+x)+l} - \frac{1}{(L-x)+l} + \frac{1}{(L+x)-l}\right]^{-1} \quad (3.11)$$

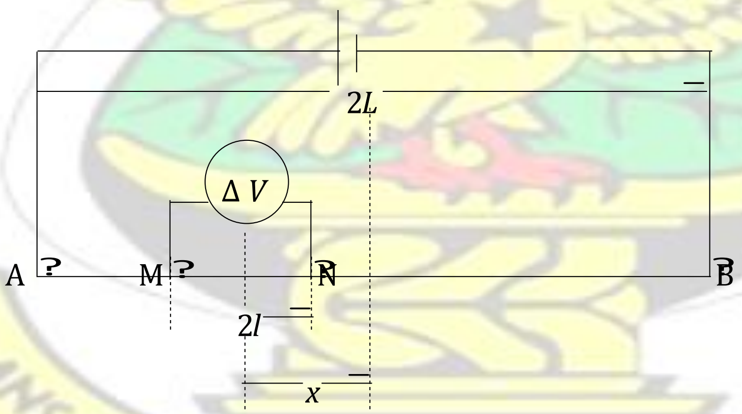

Figure 3.5: Schlumberger array (Modified from Kearey et al., 2002)

According to Telford et al. (1990), If the smallest current–potential electrode distance is always considerably greater than the distance between the two potential electrodes (by a factor of 10 or more), then ($(L - x) \gg 3l$ and equation 3.11 approximates to

$$\rho_a \approx \frac{\pi(L^2 - x^2)^2}{2l(L^2 + x^2)} \left[\frac{\Delta V}{I_i}\right] \quad (3.12)$$

For asymmetric Schlumberger array,

$$k \approx \frac{\pi(L^2 - x^2)^2}{2l(L^2 + x^2)}$$

In order to obtain a symmetrically arranged Schlumberger array where $x = 0$, equation 3.12 reduces to

$$\rho_a \approx \frac{\pi L^2}{2l} \left[\frac{\Delta V}{I_i}\right] \quad (3.13)$$

where

$$k \approx \frac{\pi L^2}{2l}$$

The Schlumberger array has advantage over the Wenner array because it penetrates deeper and resolves vertical structures better than the Wenner array.

3.1.2.3 Dipole–dipole Array

In this array, the potential pair of electrodes are placed at one end of the survey line and the current pair on the other end both maintained at the same dipole separation "*a*". Another factor "*n*"which is the ratio of the distance between C_1 and P_1 electrodes to C_2 and C_1 or (P_1 and P_2) dipole separation as indicated in figure 3.6. The dipole-dipole array is very sensitive to horizontal changes in the subsurface resistivity (resolving vertical structures), such as dykes and cavities but less sensitive to vertical changes (resolving horizontal structures) such as sills or sedimentary layers. From figure 3.6 below,

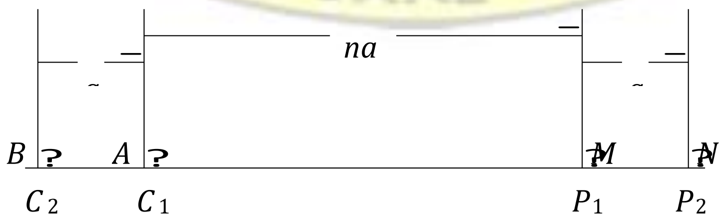

Figure 3.6: Dipole–dipole array

$|AM| = na$, $|MB| = a(n+1)$, $|AN| = a(n+1)$, and $|NB| = a(n+2)$. Substitution of these conditions into equation 3.3 gives

$$\Delta V = \frac{I_i \rho_a}{2\pi}\left[\frac{1}{na} - \frac{2}{a(n+1)} + \frac{1}{a(n+2)}\right] \tag{3.14}$$

Finding the least common multiple and simplifying further reduces the equation to

$$\Delta V = \frac{I_i \rho_a}{2\pi}\left[\frac{2}{na(n+)(n+2)}\right] \tag{3.15}$$

$$\rho_a = \pi n(n+1)(n+2)a\left[\frac{\Delta V}{I_i}\right] \tag{3.16}$$

For the dipole–dipole array,

$$k = \pi n(n + 1)(n + 2)a$$

3.1.2.4 Pole–dipole array

The pole–dipole array (figure 3.7) is an asymmetric array and one of the current electrodes is made passive and kept fixed at a large distance (infinity) from the other three active electrodes and as a result, the potential due to the fixed electrode is practically zero at the probes. The pole–dipole array has relatively good horizontal coverage and higher signal strength than the dipole–dipole array. However, when compared with the Wenner and Schlumberger arrays the signal strength of the pole–dipole array is lower.

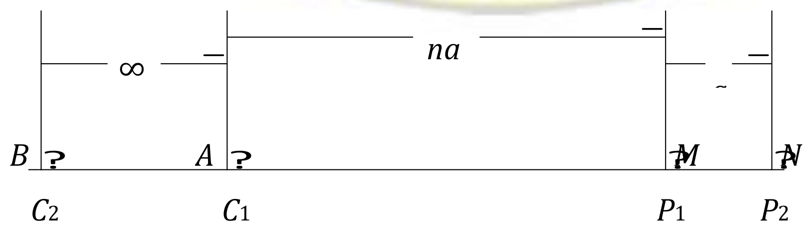

Figure 3.7: Pole–dipole array

From figure 3.7 above,

$|AM| = na$, $|MB| = \infty + na = \infty$, $|AN| = a(n+1)$, and $|NB| = \infty + na + a = \infty$.

Substitution of these conditions into equation 3.3 gives

$$\Delta V = \frac{I_i \rho_a}{2\pi}\left[\frac{1}{na} - \frac{1}{\infty} - \frac{1}{a(n+1)} + \frac{1}{\infty}\right] \tag{3.17}$$

$$\Delta V = \frac{I_i \rho_a}{2\pi}\left[\frac{1}{na} - \frac{1}{a(n+1)}\right] \tag{3.18}$$

Finding the least common multiple and simplifying further reduces the equation to

$$\Delta V = \frac{I_i \rho_a}{2\pi}\left[\frac{1}{n(n+1)a}\right] \tag{3.19}$$

therefore,

$$\rho_a = 2\pi n(n+1)a\left[\frac{\Delta V}{I_i}\right] \tag{3.20}$$

For Pole–dipole array,

$$k = 2\pi n(n+1)a$$

Among all the arrays described in this thesis, the gradient array is most suited for multichannel data acquisition, and can significantly increase the speed of data acquisition in the field and at the same time give higher data density, but it is also an attractive option for single-channel data acquisition(Dahlin and Zhou, 2006). More importantly, the high data density associated with the gradient array makes it the most preferred choice in landfill investigations because the extermination of bad data points resulting from the usual poor electrode–waste contact is compensated for during data processing. Thus a subsequent reduction in the volume of the data does not significantly affect the data. Also, the gradient array has a high signal to noise ratio though lower than the Wenner array and a good resolution for vertical structures. On the basis of the reasons elucidated above, it is expected that the objectives of the research would be achieved using the gradient array configuration.

3.2 Basic Theory of Magnetic Susceptibility Method

Magnetic susceptibility is a measure of the ease with which particular materials become magnetised under the influence of an applied external magnetic field. In rocks, it usually depends on the magnetite (Fe_3O_4), pyrrhotite (Fe_7O_8) and maghemite (γFe_2O_3) content in a given sample however, magnetite is the most common among the three (Milsom, 2003). Sedimentary rocks have the least susceptibility values followed by metamorphic and acid igneous rocks which have relatively small susceptibilities compared with basic igneous rocks which are strongly magnetic due to greater concentration of magnetite in them. Therefore the magnetic susceptibility measured in soil and rock samples, is proportional to the mass of the mineral constituents in them. Over time, activities that include weathering and erosion from rock surfaces decrease the susceptibility because the rock mass decreases and most of the magnetite component are oxidized to hematite (Milsom, 2003).

The above gives an indication that the magnetic properties of soils and rock samples are largely dependent on the presence of ironic compounds, especially in oxides and sulfides of iron. The levels of concentration of iron oxides in soils and rocks may depend on the nature, age of the soil, pedogenic and anthropogenic processes. Undoubtedly, the topsoil magnetic susceptibilities are enhanced by anthropogenically–induced sources such as road–side contamination from exhaust fumes of vehicles, ground contamination from engine oil at various repair shops, leachate contaminated grounds due to the percolation of fluids from landfill sites and various chemical applications on farm lands. The distribution of these anthropogenic contaminants has a direct relation with the distribution of magnetic susceptibility signatures in soils which depend on several factors including distance from source of pollution, wind direction, topographic elevations and depressions.

3.2.1 Classification of Magnetic Minerals

On the basis of the quantum theory, all substances are magnetic because their atoms act as dipoles due to electron spin and the orbital path of electrons around the nucleus. According to the Pauli's exclusion principle, the total number of electrons required to fill an orbit must be two with opposite spins. The spin magnetic moments for such paired electrons cancels out. The contribution of a mineral to the total magnetism of a rock and ferrous metals depend strongly on the class of mineral in them.

3.2.1.1 Diamagnetic Materials

Diamagnetic materials have all electron shells fully occupied and as such have no unpaired electrons. When placed under the influence of an external magnetic field the orbital motion of the electrons produces a magnetic field whose direction is opposite to the applied field (Kearey et al., 2002). As a result, the susceptibility of diamagnetic materials is weak and negative. Materials which fall into this class include many Earth minerals which do not contain iron, like quartz and calcium carbonate, halite, graphite etc..

3.2.1.2 Paramagnetic Materials

In paramagnetic materials the outer electron shells are partially occupied with electrons so that unpaired electrons in incomplete electron shells produce unbalanced magnetic moments. When placed in an external field the magnetic moments corresponding to the unpaired electron align themselves in the same direction to produce a weak magnetic field aligned in the same direction as the external field (Kearey et al., 2002). Paramagnetic materials such as olivine, pegmatite, gneiss, dolomite etc., have weak and positive magnetic susceptibilities but usually of order of magnitudes stronger than in diamagnetic materials.

3.2.1.3 Ferromagnetic Materials

Ferro–magnetism occurs in metals such as cobalt, nickel and iron with unpaired electrons which coupled magnetically due to strong interaction between adjacent atoms and overlap of electron orbits. The magnetic domains which are group of atoms that couple together magnetically reorient in the same direction to produce a strong spontaneous magnetisation (Kearey et al., 2002). In such materials, the strong effect produced can exist even in the absence of an external field due to their large magnetic susceptibilities. However, their susceptibilities depend on temperature and strength of applied field. Consequently, ferro–magnetism disappears and behaves as paramagnetic if the materials are heated to their Curie Temperature as inter-atomic coupling is restricted and domains ceases to exist.

3.2.1.4 Antiferromagnetic Materials

In antiferromagnetic minerals such as haematite, magnetic domains form but align in antiparallel fashion with equal numbers of dipoles in each direction so that magnetic field cancels out. However, defects in the crystal lattice structure of an antiferromagnetic material may cause small net magnetisation in response to an applied external field (Kearey et al., 2002). Consequently, the magnetic susceptibility for such materials are large and positive.

3.2.1.5 Ferrimagnetic Materials

In ferrimagnetic materials such as magnetite, titanomagnetite, pyrrhotite etc., the magnetic domains are similarly antiparallel, but of unequal magnitude in each direction. Consequently ferrimagnetic materials can produce a strong net magnetisation in the presence of an external field (Kearey et al., 2002). In such materials susceptibilities are large and positive and as such, magnetic domains can permanently align to produce a strong spontaneous magnetisation that still exists after removal of external field. Like ferromagnetic materials, ferrimagnetism disappears when heated above the curie temperature.

3.3 Basic Theory of Magnetic Gradiometry

Magnetic surveys explore for spatial variations in the magnetic field of the Earth that are caused by magnetised rocks and buried ferrous metals as a result of measurements of total magnetic intensities (TMI) at or near the Earth's surface. The local perturbations (anomalies) in the TMI at various stations are caused by the contributions of both induced and remanent magnetisations. This is mainly due to the fact that the magnetic properties of rocks are acquired either by induced magnetisation under the influence of the geomagnetic field or remanent magnetisation due to the effect of the Earth's magnetic field when the rocks last cooled during their formation through a process called magmatic differentiation.

3.3.1 Induced magnetisation

When magnetic minerals in rocks or ferrous materials in MSW are under the influence of an external magnetic field, secondary magnetism is induced in them. The secondary magnetism induced in such materials is called induced magnetisation $\vec{J}_i$ and for low magnetic fields, it is proportional to the magnetising field $H\sim$ of the external field. When the applied field is removed the induced magnetisation disappears because the magnetic domains in the materials rotate back to their original orientations. The ratio between the induced magnetisation and the inducing field is expressed as

$$\chi_m = \frac{\vec{J}_i}{\vec{H}}$$

where χ_m is the magnetic susceptibility. It is a dimensionless quantity and can take both positive and negative values. Positive values of χ_m imply that the induced magnetic field, $\vec{J}_i$, is in the same direction as the magnetising field, $H\sim$ whiles the negative values imply that the induced magnetic field is in the opposite direction as the magnetising field. For the same rock, the magnetic susceptibility values may differ slightly because the distribution of the minerals within the rock may not be uniform.

3.3.2 Remanent magnetisation

Primary remanent magnetisation is a phenomenon by which rocks can become permanently magnetised in the geomagnetic field during the formation of a rock. It consists of:

- *Thermoremanent magnetisation* (TRM), which results when ferro or ferri–magnetic magnetic materials are cooled below the curie point in the presence of the geomagnetic field so that their particles become oriented in the direction of the Earth's magnetic field at that time.

- *Detrital remanent magnetisation* (DRM), which is acquired when fine–grained magnetic particles settle slowly during formation of sedimentary rocks in the presence of the geomagnetic field and that the settling particles are oriented by Earths magnetic field at that time.

Secondary remanent magnetisation refers to magnetisation acquired later in a rocks history by alteration processes. It also comprises of:

- *Chemical remanent magnetisation* (CRM), which is acquired in situ when magnetic minerals grow or are chemically altered to another form below Curie temperature.

- *Viscous remanent magnetisation* (VRM) is acquired by long exposure to ambient field in uniform environment.

- *Isothermal remanent magnetisation* (IRM) is acquired over a very small time in a strong magnetic field at constant temperature.

3.4 Principle of Operation of the Proton Magnetometer

The proton precession magnetometer is made up of a cylindrical container or bottle sensor component, usually filled with proton–rich liquid like kerosene, water or alcohol and wrapped with metallic coil. The sensor is connected by means of a cable to a small unit called 'console'which houses a battery, amplifier, electronic switch and a frequency counter as shown in figure 3.8A. Each proton possesses both magnetic moment and angular momentum as it is always in motion. In the presence of the Earth's magnetic field, most of the protons align themselves parallel with the direction of the applied field and the remainder anti–parallel to it (figure 3.8B) so that the net magnetic moment acquired is in the direction of the Earth's

field.

When the switch is closed, a momentary DC current is supplied by the battery through the coil surrounding the liquid to generates a perpendicular and relatively stronger magnetic field than that produced by the Earth's field (figure 3.8C). The protons assume a new magnetic direction along that of the applied field. When the momentary power is cut to the coil by opening the switch, a torque is generated by the Earth's magnetic field on the aligned protons and they begin to precess around the direction of pre–existent Earth's total field (figure 3.8D) at a frequency proportional to the Earth's magnetic field strength (equation

3.21). Because protons are charged particles, their precession around the pre–existent Earth's field produces a time–varying magnetic field that induces alternating current AC in the coil surrounding the sensor bottle whose frequency is equal to the precession frequency of the protons.

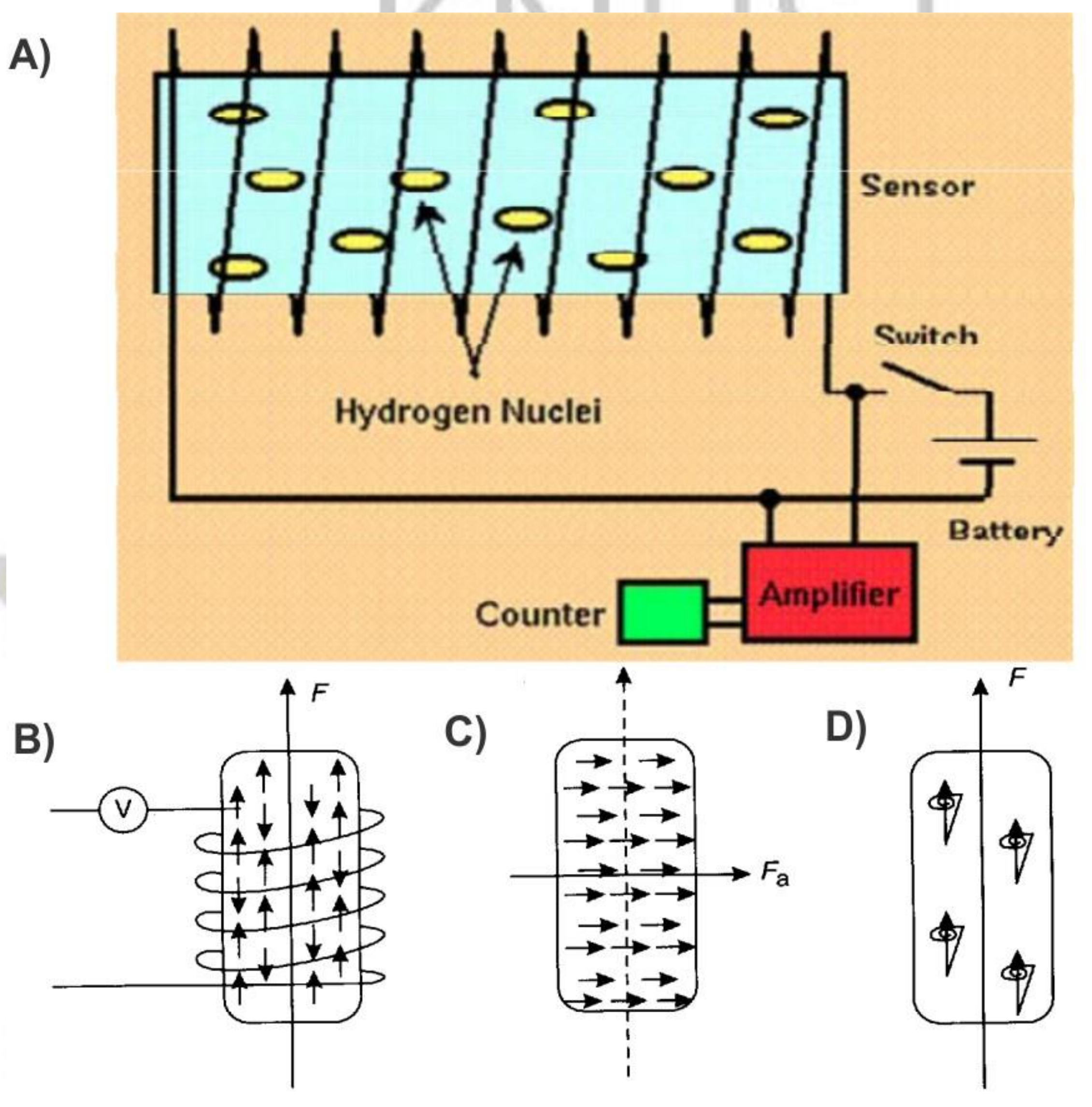

Figure 3.8: A) A bottle sensor containing hydrogen nuclei (protons) wrapped with a coil and connected to the console. B) Protons oriented parallel and anti–parallel to the Earth's field. C). Protons aligned perpendicular to the Earth's field. D). Protons precessing around the Earth's field (modified from Kearey and Brooks (1991))

$$F = \frac{2\pi f_p}{\Phi_p} \tag{3.21}$$

where F is the Earth's magnetic field strength f_p

is the precession frequency and

Φ_p is the gyromagnetic ratio of the proton, which is the ratio of the magnetic moment to the spin angular momentum of the proton. The total field strength can be accurately determined because the constant of proportionality is well known.

3.5 Total Magnetic Intensity (TMI)

The magnetic method is based on the fundamental principle that when a magnetic material is placed within the Earth's magnetic field, it develops an induced magnetic field. The induced field is superimposed on the Earth's field at that location creating a magnetic anomaly. Thus, the measured total magnetic intensity $B\sim$, measured in Tesla (T) is the sum of the magnetising field strength (Earth's field) $H\sim$ and induced field $\vec{J}_i$.

$$\vec{B} = \mu_o(\vec{H} + \vec{J}_i) \tag{3.22}$$

where μ_o is the permeability of free space of value $4\pi \times 10^{-7}$ H/m. Substituting $\vec{J}_i = \chi_m \vec{H}$ into equation 3.22 gives

$$B\sim = \mu_o(H\sim + \chi_m H\sim)$$

$$B\tilde{} = (\chi_m + 1)\mu_o H\tilde{}$$

$$B\sim = \mu_r \mu_o H\sim$$

where

$$\mu_r = (\chi_m + 1)\ B\sim$$

$$= \mu H\sim$$

where μ is permeability of the medium and μ_r is the relative permeability given by $\mu_r = \frac{\mu}{\mu_o}$

3.6 Magnetic Data Enhancement

Generally, the interpretation of magnetic data and anomalies is complex as the magnetisation due to a subsurface materials results from the combined effect of two vector magnetisations, induced and remanent, that may have different magnitudes and directions. For example, the ambient field is vertical and axisymmetric with anomalies produced by bodies whose magnetisations are solely due to induced magnetisation (Kearey et al., 2002). However, the existence of remanent magnetisation direction may cause the anomalies to be displaced from their causative sources.

Again, when sources of induced magnetisation are observed at the poles the intensity and amplitude of the magnetic anomalies are greater in comparison to similar structures at lower magnetic latitudes. This is because the Earth's field intensity is strongest at the poles and for that matter increases from the equator to the poles. The effect is that structures with low magnetic anomalies recorded at the poles are represented with higher ones compared with similar structures at lower latitudes. For this reason, a range of mathematical enhancement operators can be specified to make accurate interpretations.

3.6.1 Reduction to the Pole (RTP)

Reduction to the pole is an important component of magnetic data processing, especially when one is surveying on a large scale. The dipolar nature of the Earth's magnetic field causes a horizontal displacement of the measured anomaly from the exact source location. The RTP operator can transform a magnetic anomaly caused by an arbitrary source due to induction into the anomaly that the same source would produce if it is located at the pole.

In the case where induced magnetisation of magnetic sources is assumed, the amplitude correction using a simplest and effective frequency domain technique was calculated by (Grant and Dodds, 1972) as expressed in equation 3.23. However, the amplitude correction at low magnetic latitudes unreasonably amplifies noise and distorts magnetic anomalies from sources magnetised in directions different from the inducing field. This makes the RTP transformation unstable at low magnetic latitudes. The reduction to the pole operator is expressed as

$$L(\theta) = \frac{1}{[\sin(I) + i\cos(I)\cos(D - \theta)]^2} \tag{3.23}$$

where θ is the wave number direction, I is the magnetic inclination D is the magnetic declination.

3.6.2 Analytic Signal

Unlike the RTP operator which amplifies and distorts the magnetic anomaly at low latitudes, the analytic signal operator which is another form of RTP addresses the problem of interpreting the total magnetic field anomalies at lower latitudes through the use of 3–D analytic signal amplitudes applied to the magnetic data (Nabighian, 1972; Roest et al., 1992). The amplitude of the analytic signal of the total magnetic field produces maxima over magnetic contacts regardless of the direction of magnetisation (Macleod et al., 1993). The application of the analytic signal operator transforms the total field magnetic anomaly by removing the skewness associated with magnetic data. In doing so, the anomalies are made to overlie the source for easy and accurate interpretation. This property of the analytic signal has aided in edge detection (Nabighian, 1972) and depth estimation using the amplitude half–

width rule Roest et al. (1992) in magnetic surveying. Roest et al. (1992) showed that the amplitude of the analytic signal can be derived from a three dimensional orthogonal gradient of the total magnetic field using the expression below.

$$|A(x,y)| = \sqrt{\left(\frac{\partial M}{\partial x}\right)^2 + \left(\frac{\partial M}{\partial y}\right)^2 + \left(\frac{\partial M}{\partial z}\right)^2} \tag{3.24}$$

where $A(x,y)$ is the amplitude of the analytic signal at (x,y), M is the observed total field intensity at (x,y),

Chapter 4

SITE DESCRIPTION, MATERIALS AND METHODS

4.1 Project site Description

4.1.1 Location

The study area is located in Sunyani municipality and it is about 2.5 km from the city centre. Sunyani is the capital of Brong-Ahafo Region located in the middle belt of Ghana and about one–third of the total land area not being inhabited. The region shares local borders with the Northern, Volta, Ashanti and Western Regions. It shares a common border internationally with La Cote Divoire. Sunyani municipality is one of the twenty–seven administrative districts in the Brong Ahafo Region of Ghana. It covers a large land area of 506.7 km^2 which lies between Latitude $7^o20'$ N and $7^o05'$ N and longitudes $2^o10'$ W and $2^o30'$ W. It is bordered on the north by Sunyani West District, west by Dormaa East District, south by Asutifi District, east by Tano North District (SMA, 2010).

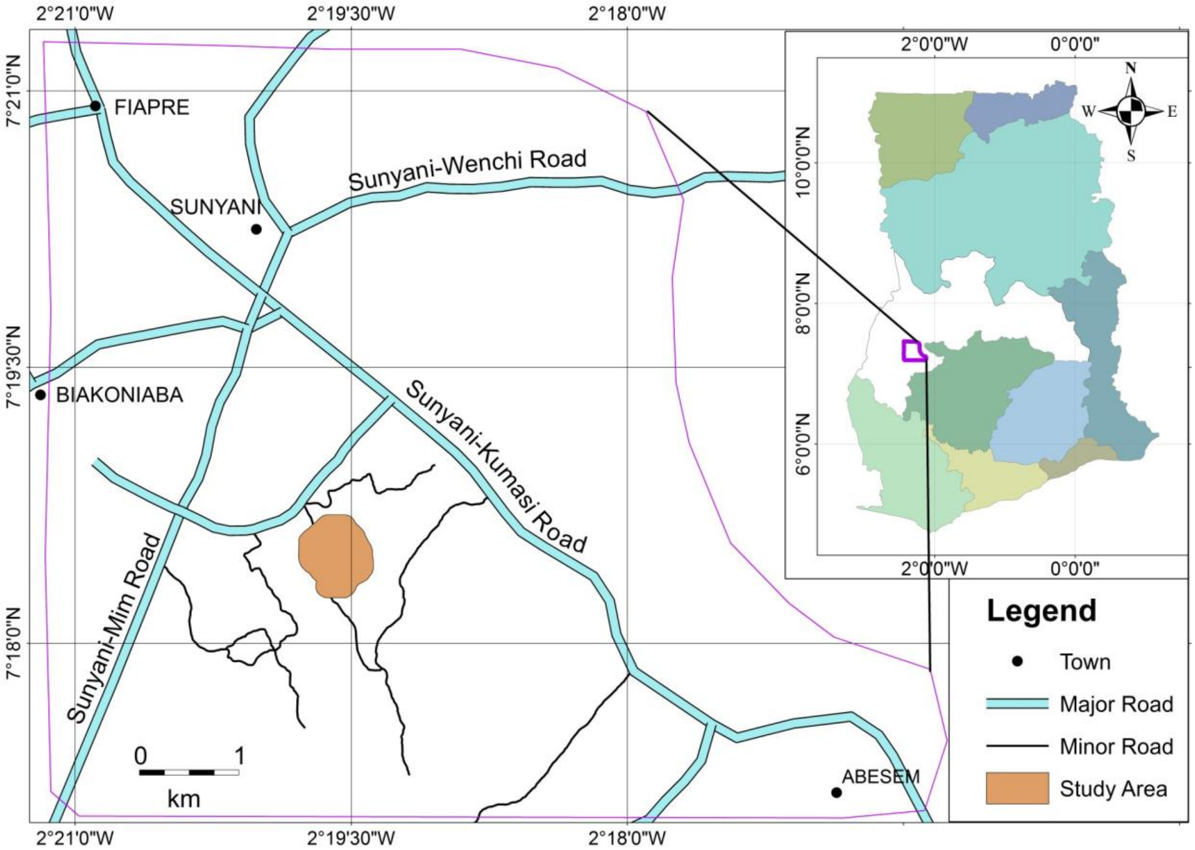

Figure 4.1: Map of Sunyani Municipality Showing the Study Area

4.1.2 Topography and Drainage

The Sunyani Municipality falls within the middle belt of Ghana with elevations ranging from 229 m to 376 m above the mean sea level. It is characterised by a moderately flat topography which makes it conducive for large scale agricultural mechanization in the area. The drainage in the municipality is dendritic with several streams and rivers. Notable among them are the Kankam, Amoma, Benu, Bisi, Yaya and Tano rivers. These surface waters are seasonal hence, water shortage is paramount during harsh (dry) seasons (SMA, 2010).

4.1.3 Climate and Vegetation

The study area falls within the semi–equatorial climatic zone of Ghana. The monthly temperature varies between 23 °Cand 33 °Cwith the lowest around August and the highest observed around March and April. The relative humidities are high averaging between 75 and 80 percent during the rainy seasons and below 70 percent during the dry seasons of the year. This offers two farming seasons in a year which support agricultural production in the municipality. The average rainfall for Sunyani Municipality between the years 2000 and 2009 was about 88.99 cm. The district experiences double maxima rainfall pattern with the main rainy season between March and September and the minor between October to December which makes Sunyani ideal for vegetative growth. The municipality falls largely within the moist-semi deciduous forest vegetation zone. This vegetation zone contains most of the valuable timber species. The existence of the vegetation cover makes cocoa and citrus thrive well in the municipality. There are two major forest reserves in the municipality and they are the Yaya and Amoma forest reserves (SMA, 2010).

4.1.4 Economy of the study Area

The economy of the municipality used to be predominantly agrarian with majority of the working class involved in crop farming, animal husbandry and fishing. However, the upsurge of commercial, industrial and service activities is a manifestation of potential diversification of the local economy. According to the Population and Housing Census 2010, the total population of Sunyani Municipality stood at 123,224 representing 5.3 percent of the regions total population (GSS, 2014). Currently the service sector employs majority (58.3%) of the population in the Municipality.

4.2 Geology

4.2.1 Local

The Sunyani Municipality is geologically underlain by Precambian rocks of Birimian formations.

It is associated with extensive masses of granite predominantly those of the basin type granitoids. The Birimian and its associated granites as well as the Dahomeyan belong to the basement crystalline rock which is one of the two major formations dominant in the geology of Ghana making up 54% of the land area of the country. The basement crystalline rocks are of precambian age comprising gneiss, granite–gneiss, phyllite, schist, quartzite and migmatite. Other subdivisions of this basement complex include the Togo, Buem and Tarkwaian rock formations

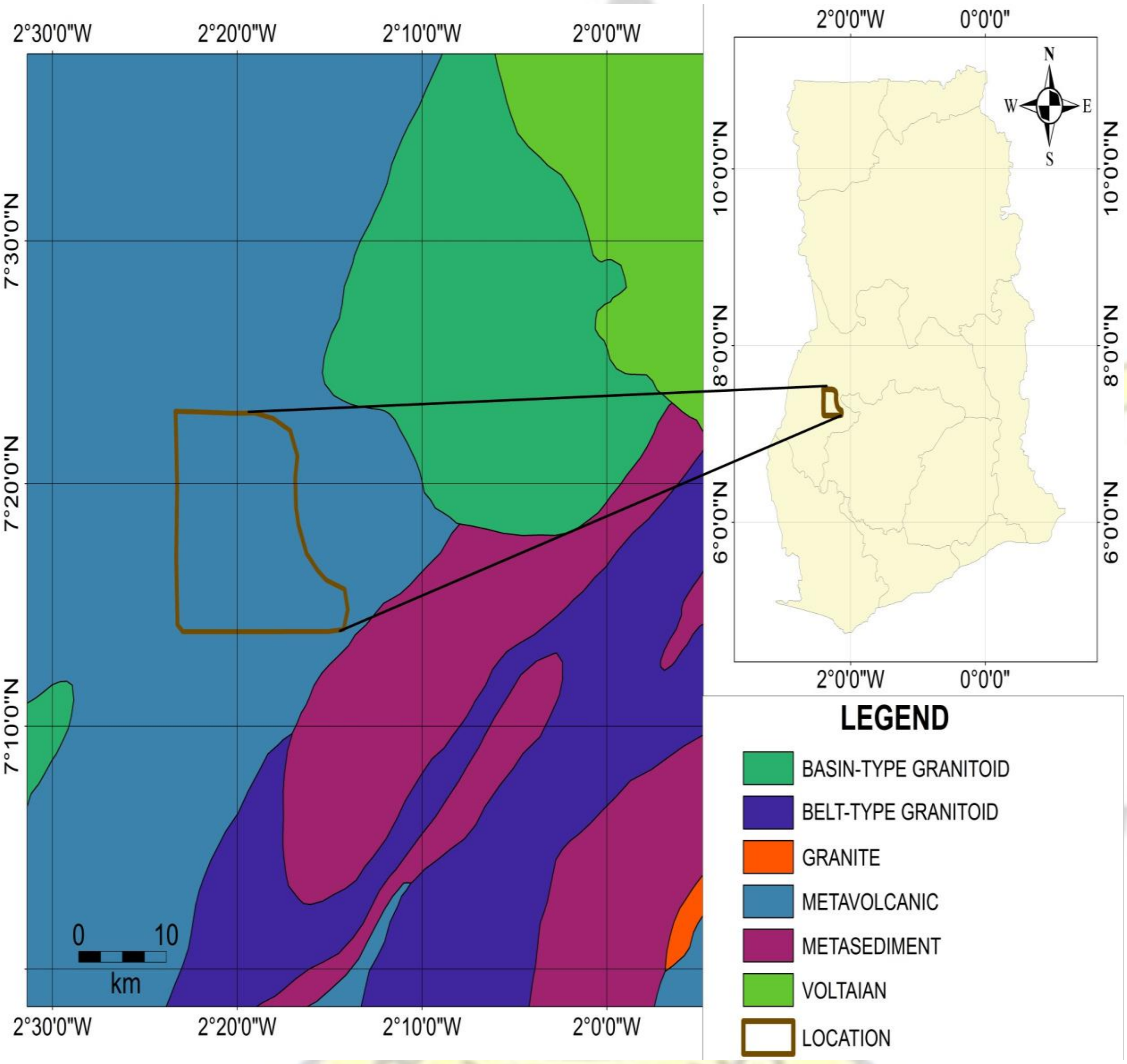

Figure 4.2: Geological Map of Sunyani

4.2.1.1 The Birimian Supergroup

Rocks of the Birimian System predominantly underlie the southern, western and northern parts of Ghana. They host most of the gold and diamond deposits in Ghana for which reason they have been subjected to considerable study for mineral exploration. The Birimian Supergroup is a series of metamorphosed basic volcanic and sedimentary units consisting of two main divisions namely, the Metavolcanics (Upper Birimian) and Metasediments (Lower Birimian). The Metasediments consist of tuffs, greywackes and phyllites whilst the Metavolcanics comprise mainly of volcanic and pyroclastic rocks (Junner, 1935). The

Birimian rocks are believed to have undergone changes during active tectonics during the Eburnean event between 2150 and 1850 Ma. The rocks are folded, metamorphosed and intruded by granitoids as a result. The tectonic sequence of the Eburnean event are contributing factors to the structure in the Birimian Supergroup even though the beginning of the Eburnean is not fully understood. This is also because there are no basement rocks to show the underlying materials upon which the initial Birimian rocks were laid (Leube et al., 1990). Three phases of felsic intrusives intruded the Birimian Supergroup during this Eburnean event. The first phase being the Birimian sedimentary rocks were intruded by the basin type (Cape Coast) granitoids which are considered to be syn-tectonic intrusions because of the presence of well-developed foliations (Milesi et al., 1990). The second phase which is the Birimian volcanic rocks were intruded by the belt type (Dixcove) granitoids according to Kesse (1985) and are considered to be post–tectonic intrusion, because of the absence of foliation (Milesi et al., 1990). The third phase found within the metasedimentary basins consists of K-rich granitoids also known as the Bongo granitoids (Leube et al., 1990). For economic purposes, the Birimian makes up the most important geologic group (Cudjoe, 1961). Rocks of the Birimian Supergroup are not permeable so groundwater occurrence in this formation is associated with the development of secondary porosity which results from chemical weathering and fracturing. Hence, groundwater occurrence is found in these fractured zones.

4.2.1.2 Granitoids

The granitoids form a very significant portion of the Main Shield which occupies the southernmost part of the West African Craton. Two main granitoids are predominant in the study area namely, the basin type granitoids and the belt type granitoids.

- The basin type granitoids in the metasedimentary basin and the belt type granitoids in the volcanic belt intruded the Birimian rocks in about 2.1 Ga ago during the Eburnean Orogeny. The basin type granitoids which are mostly batholitic in nature tends to coincide with the central axes of the sedimentary basin (Leube et al., 1990).

- The belt type granitoids are typically hornblende–bearing and are commonly associated with gold mineralisation where they occur as small plutons within the volcanic belts. They are mostly elongated and often unfoliated plutonic rocks. They are also made up of quartz diorite, granodiorite, trondhyemites, tonalite, granite etc..

4.3 Instrumentation and Materials Used

The study involved the integration of three geophysical methods namely, magnetic susceptibility, ground magnetic gradiometry and electrical resistivity tomography for the characterisation of the Sunyani municipal waste disposal site near Asufufuo. The integration of these three geophysical methods was expected to remove some of the ambiguities that are associated with any single method in order to better characterise the waste disposal site. The various instruments used for the study are the ABEM LUND Resistivity Imaging System, the

Bartington MS2 Susceptibility System and the GEM Gradiometer System, GPS and processing softwares such as arc–gis, geosoft, res2dinv and mapinfo respectively.

4.3.1 Description and Operation of the Bartington MS2 Equipment

The geophysical equipment that was used for magnetic susceptibility measurements is the Bartington MS2 Susceptibility System which consists of a MS2 meter that is connected to the MS2D loop sensor that is in turn attached to a handle with an electronic unit as shown in figure 4.3b.

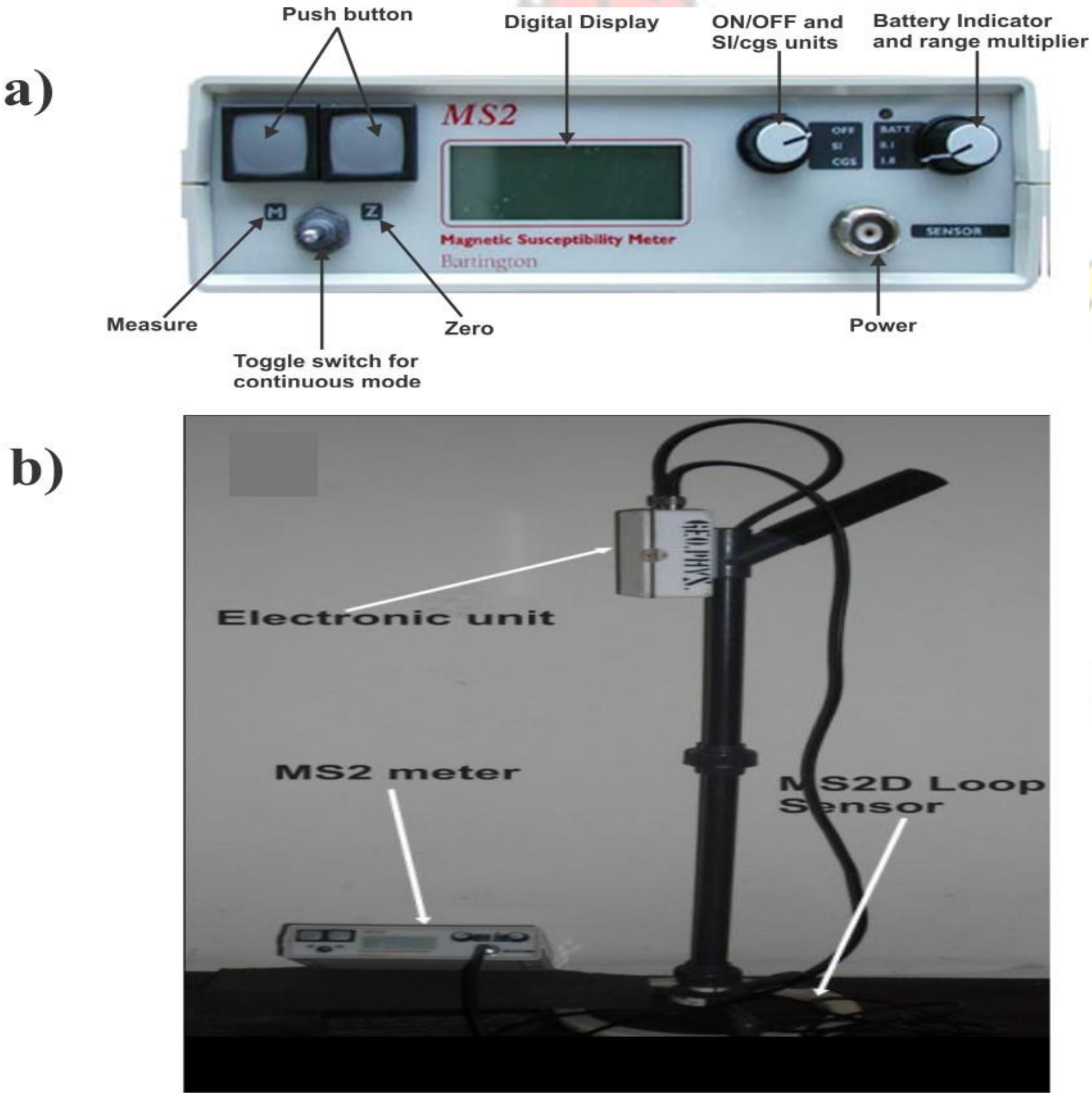

Figure 4.3: The Bartington MS2 Susceptibility System Comprising of a) MS2 Meter Assembled with b) Electronic Unit, MS2 Loop Sensor and the Handle

It is used for rapid measurement of the amount of magnetic minerals in the top 100 mm of the subsurface and according to Lecoanet et al. (1999), 90% and 95% of the susceptibility signal comes from the top 6 cm and 8 cm of the subsurface in the case of the MS2D search sensor. The MS2D search loop sensor is 185 mm in diameter and is designed to make surface magnetic susceptibility measurements of soils, rocks and stream channels in various field surveys (Dearing, 1999). The loop allows the bulk susceptibility of a circular area of diameter of about 185 mm to be quickly measured. The sensor contains a coil that generates an AC magnetic field to magnetise materials placed around it based on their magnetic susceptibilities. The meter measures this and displays the value of susceptibility on the digital display. It is a simple equipment, quick to use and is mainly deployed in mapping and reconnaissance surveys.

4.3.2 Description and Operation of the Proton Gradiometer

The equipment used for the gradiometric measurement is the GEM systems which is made up of the GSM–19TGW console, one sensor for magnetometer and two for gradiometer, radio frequency cable, download cable, shoulder harness, sensor mounting rods, and RS–232 cable, GPS and GPS support rod as assembled in figure 4.4. The console with all electronic circuits has 16 key keyboard with B serving as ON switch, graphic display (64 x 240 pixel), sensor and power connectors. The sensors are dual–coils designed to reduce noise and improve gradient tolerance. The coils are electrostatically shielded and contain a special proton rich liquid in a sealed pyrex bottle radio frequency (RF) resonator.

The gradiometeric survey was carried out using the two sensors of the GSM–19TGW Proton Precession Magnetometers having a sensitivity of 0.05 nT. The two sensors were mounted on a sensor mounting rod with a vertical separation of 56 cm. The console is configured in

Figure 4.4: The Gradiometer

gradient mode (with two sensors mounted on a vertical staff at a distance of 56 cm apart as shown in figure 4.4). The mounted GPS also vertically separated from the sensors was used to obtain the geographic coordinates during the data acquisition. The top sensor measures the strength of the Earth's magnetic field and that of the bottom measures the strength of the Earth's field as altered by any near–surface magnetic signatures. The difference in the magnetic intensities as measured by the top and bottom sensors allows the instrument to "correct "for the strength of the Earth's magnetic field so that it "reads "only the local deviation. The effect is that time–dependent variations such as diurnal variations in the data are completely eliminated. The difference is divided by the distance of separation between the two sensors and ultimately expressed in nanoTeslas per metre (nT/m). Thus the console keeps records of the ambient magnetic field strength as measured by the bottom sensor and that as obtained by the difference in the measurements by the two sensors.

4.3.3 Description of the ABEM LUND Resistivity Equipment

The setup of the ABEM LUND Resistivity Imaging System as indicated in figure 4.5 comprising of ABEM terrameter SAS 4000 equipment, electrode selector, a 12 V car battery, cable jumpers, steel electrodes and the Lund cable spread was used for the electrical resistivity data collection. There are four Lund cable spreads each with 21 take-outs using 2 m electrode separation. When all the four cables are connected, the total length is 160 m and could probe to a depth of about 30 m.

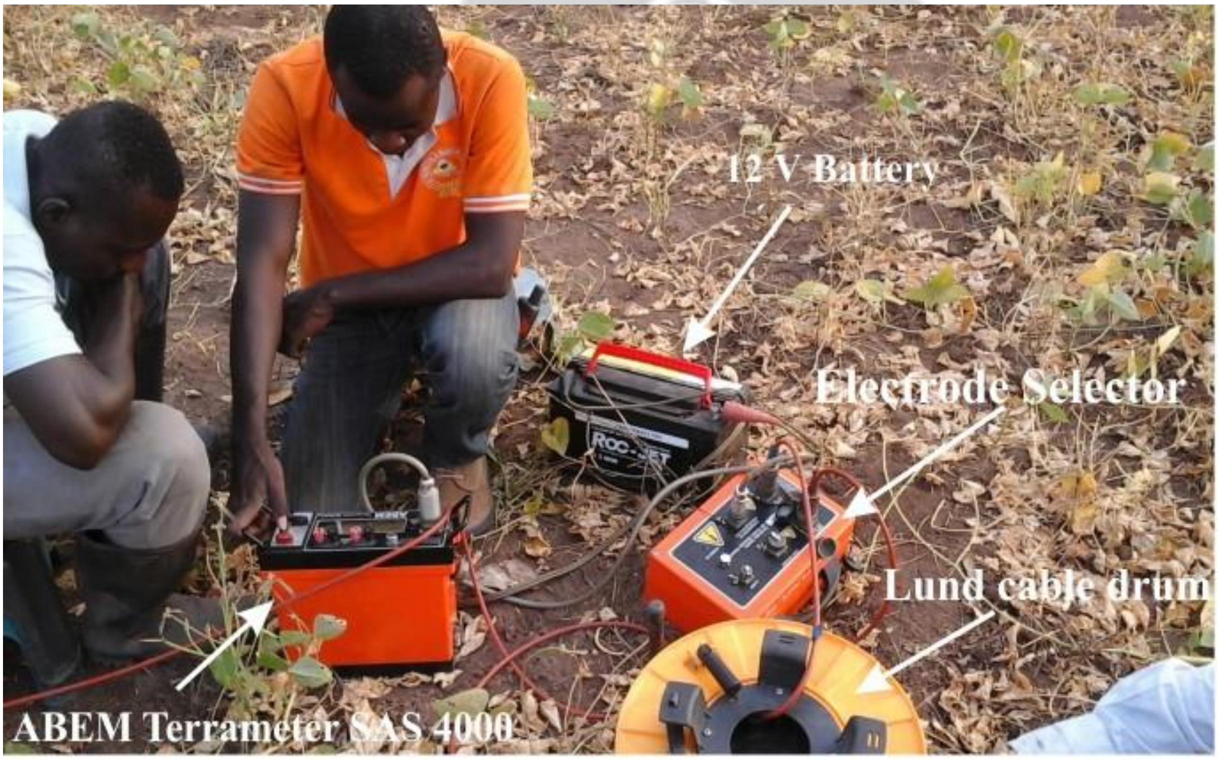

Figure 4.5: Set up of ABEM LUND Resistivity Imaging Equipment

4.4 Field Procedure and Data Acquisition

4.4.1 Magnetic Susceptibility Measurements

The Bartington MS2 Susceptibility System comprising of the MS2 meter, MS2D search loop sensor, electronic unit attached to the handle was assembled as shown in figure 4.3b above. The meter was switched on and set in SI units while the sensor was in low frequency mode which is normally selected for single frequency measurements. The measuring range of 1.0 was selected and the M/Z toggle switch centred. The sensor was zeroed by holding the sensor in the air, at least 100 cm away from other objects, and pushing the Z button. The meter display was cleared and by pushing the M button, air measurements were taken. The sensor was placed on a body or surface whose magnetic susceptibility measurement was to be taken and the M button pushed to obtain a reading. Magnetic susceptibility measurements were taken at 5 m intervals along these profiles. In order to minimise error due to instrumental drift, the meter was zeroed at regular intervals.

4.4.2 Magnetic Gradiometry Method

The whole GEM system consisting of a charged battery inside the GSM–19TWG console, two sensors, GPS was assembled (*see* figure 4.4). The console was powered on, configured in gradient mode under survey menu and GPS initialised. Ground magnetic measurements were made with the gradiometer at regular intervals of 5 m as the waste was traversed many times along designate profiles to cover the entire waste stretch. Measurements were also extended to cover at least 50 m away from the periphery of the main waste. Intense fields from man–made electromagnetic sources like power transmission lines and other sources of noise like buildings, watches belt buckles etc., were avoided in the survey.

4.4.3 Electrical Resistivity Tomography

On each straight profile, the first three Lund cables were laid and steel electrodes were well hammered into the ground at each take–out point so that electrodes and the Lund cables were connected via electrode cable jumpers. The electrode selector was then connected to the end of the first Lund cable and the beginning of the second Lund cable whiles a connector was used to link the second and third Lund electrode cable with the groove facing the equipment. In each case it was ensured that the last and the first electrode take–out overlapped by connecting them to the same electrode. The ABEM terrameter SAS 4000 equipment was set up by connecting it to a charged battery and the electrode selector.

The gradient array configuration was used for the data acquisition and the GRAD4LX8 and GRAD4S8 protocols were selected. For the GRAD4LX8 protocol (long layout), all the three cables were used and only the odd-numbered electrodes were connected for the measurements. The electrode separation used for this protocol was 4 m. For the GRAD4S8 protocol (short layout), only the inner cables were employed for the measurements and all the take-outs were used with a take-out separation of 2 m.

In all, thirty one (31) steel electrodes were fixed into the ground with the aid of small hammer at 4 m spacings for the first three cables respectively to attain a horizontal length of 120 m for the first set of measurements using the GRAD4LX8 protocol. The electrode resistance test was run first before the measurements to ensure that all the thirty one (31) electrodes had all been connected and were conducting. In some cases the electrode test failed and water had to be poured on those electrodes and they were also hammered deeper to ensure they pass the electrode test. At the same time as the measurements of the GRAD4LX8 was going on, twenty (21) electrodes were fixed mid–way in-between the electrodes of the first and second cables for the GRAD4S8 measurements.

The GRAD4S8 measurements were carried out after measurements for the GRAD4LX8 protocol had finished. Electrode test was also carried out for this short layout of forty one electrodes spaced 2 m apart (total length 80 m) before the measurements were carried

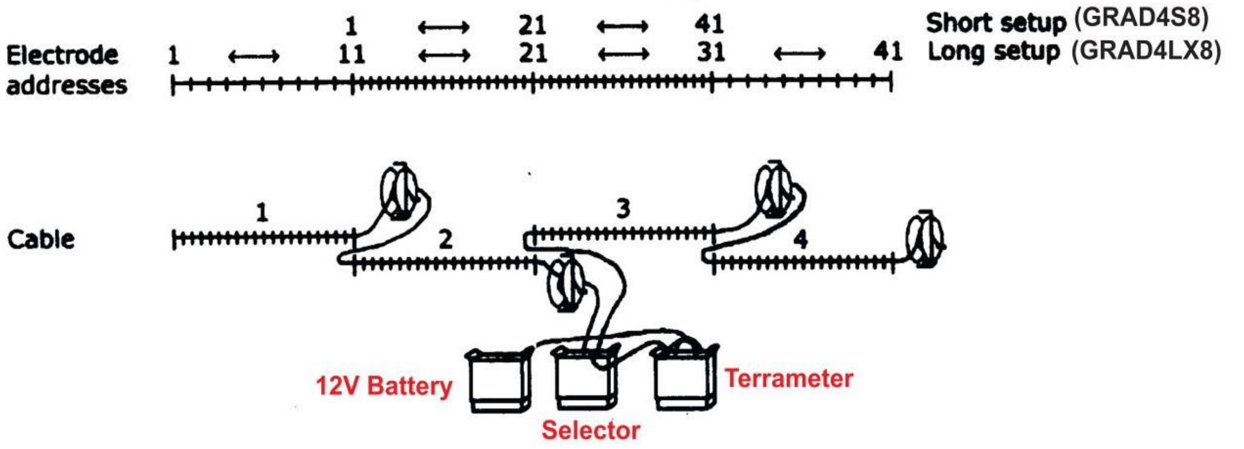

Figure 4.6: Electrode lay–out for GRAD4LX8 and GRAD4S8 protocols. (Modified from (ABEM Instrument AB, 2008))

out. After the GRAD4S8 measurement, the terrameter equipment, electrode selector and the 12 V battery were moved to the next station. The terrameter and selector were then connected between the second and third cable. The connectors were used to connect first and second cables and the third and fourth cables in each case with the groove on the cable joint pointing to the station. The procedures described for the first set of measurements were repeated to acquire the data but this time, the entire spread of length 160 m was used for the GRAD4LX8 (long lay–out) protocol. For the GRAD4S8 (short lay–out) this time, the twenty (20) electrodes were fixed mid–way in-between the electrodes of the second and third cables as indicated in figure 4.6. The profiles had a minimum electrode spacing of 2 m, and a minimum profile length of 160 m. The roll–along technique was used in collecting data on profiles which were longer than 160 m in order to cover the entire length of all the six profiles where necessary. This was done by moving the first cable from the setup to connect to the end of the setup to form another four cable setup. In order to account for the effects of topography during the data processing, the hand–held GPS was used to locate the positions and elevations of the electrodes taken at approximately 20 m intervals along each profile line and the data were incorporated to the resistivity data in deriving a subsurface electrical resistivity distribution model.

4.5 Data Processing and Representation

4.5.1 Magnetic Susceptibility

Recent development in the display, processing and interpretation of magnetic data has been extremely beneficial especially, when large data sets are involved over large survey areas. By convention, large data sets were displayed as a contoured anomaly map but the advent of digitised computer software technology in the early 1970s has made it possible to process data previously recorded in analogue form (Milsom, 2003). Instead of contouring, the surveyed area covered is divided into equal square cells called *grids* each of which is assigned a magnetic susceptibility value, ambient field strength value or magnetic gradient value in the case of the gradiometer. In the case of the geosoft software, the *grid cells* are manipulated and displayed as individual pixels that represent a colour image which portrays blue as negative anomaly and red as positive anomaly. The different colour shades represent varying degree of magnetic signatures such that purplish–red or magenta indicates high–amplitude positive anomaly while deep blue, a high–amplitude negative anomaly.

The magnetic susceptibility data sets were enhanced by the Geosoft (Oasis Montaj) application software for fast and easy interpretation. It involved building a database (project) in excel spread sheet from the acquired field data and importing into the main Geosoft database. The geophysical data sets as well as their corresponding geographic coordinates were acquired at each station as the waste body was traversed. The geographic reference positions in terms of elevation, longitude and latitude and the corresponding magnetic susceptibility measurement at each surveyed station were assigned to columns in excel spreadsheet and saved in csv format as magsus.csv. The file was then imported into the Oasis Montaj (Geosoft) as a database. The Universal Traverse Mercator (UTM) projection with zone 30N was used. Projections were then set and the minimum curvature algorithm was applied to grid the data to produce a grid map for the elevation and magnetic susceptibility columns in the database.

4.5.2 Magnetic Gradiometry

The geographic reference positions in terms of elevation, longitude and latitude and the corresponding magnetic gradient and Total Magnetic Intensity (TMI) measurements at each surveyed station were assigned to columns in excel spreadsheet and saved in csv format as grad.csv. In the gradiometric data processing, similar procedure described in the above section was applied to the data. The column corresponding to the magnetic gradient was gridded to produce a magnetic gradient anomaly map for the study area. In order to enhance the data by removing the effects of the remanent magnetisation on magnetic anomaly obtained at points of low magnetic latitude, the analytic signal filter under the MAGMAP menu was applied to transform the magnetic data. This operation removes the noise associated with the magnetic data due to the north–south component of the geomagnetic field which portrays points of low magnetic susceptibilities with high magnetic anomaly and vice versa. Finally, a base map was generated and a horizontal colour bar was also activated to describe the map.

4.5.3 Electrical Resistivity

The results of resistivity measurements is an apparent resistivity which are used in an inversion software program to give the distribution of electrical properties of the subsurface. The data are presented as 2-D profiles of electrical resistivity distribution called pseudo-sections. Retrieving the data from the terrameter was made possible by the terrameter SAS 4000 utility software. The files inside the terrameter are saved in binary format with file extension .S4K. The retrieved files were then converted into a RES2DINV output data files for them to be inverted using th RES2DINV software. The data files were first read into the RES2DIV software and bad data points which are usually occur as spikes in the data were exterminated from the data and the resulting files was saved. The bad data points could be due to the failure of the relays at one of the electrodes, poor electrode–ground contact due to dry, sandy or stony ground, attaching electrodes to wrong connectors (Aning et al., 2013). The edited files were opened to include the various elevations recorded with the hand held GPS on each profile line and the results saved. The edited files that had been incorporated with topography were reread into the RES2DINV software and the least squares inversion based on the robust inversion routine was used to invert the data. A minimum contour value of 5.0 and a user defined contour increase factor of 1.659 were specified. This generated even contour values and spacing on the resistivity models for all the profiles for easy comparison.

Chapter 5

RESULTS AND DISCUSSION

5.1 Results

5.1.1 Introduction

This chapter brings into perspective the results obtained from the research and the deductions made herein. It also discusses the suitability of each of the three geophysical methods to the realisation of the stated objectives in waste disposal site characterisation. The non–invasive, fast and cost–effective ERT, magnetic susceptibility method and magnetic gradiometry in waste disposal site characterisation have proven to preserve the competence, geometries, orientations and integrity of the background geologic materials and therefore show unlikely tendencies of disturbing them as opposed to traditional drilling and other exploratory excavations that can pose potential threat to the subsurface materials. For example, drilling can create fractures in rocks which serves as conduits for leachate migration and accumulation at various waste disposal sites. The three datasets acquired by the above methods were used to determine potential zones of leachate contamination and accumulation around the waste disposal site, delineate preferential leachate migration pathways and their vertical and lateral extent in the groundwater system, determine the composition and thickness of the waste and to delineate the boundaries of the waste at the waste disposal site.

In the data acquisition process, a total of 1,295 volume susceptibility measurements were taken with minimum and maximum readings of 1.0×10^{-5} SI and 9890×10^{-5} SI. Generally, very high volume magnetic susceptibility values were recorded on the main waste body and moderately high values were observed at the immediate vicinity of the waste deposit while relatively low susceptibilities were obtained farther from the waste body. On the whole, an average value of 1247×10^{-5} SI was observed over the study area.

In a similar survey using the gradiometer, a total of 1546 gradiometeric measurements were obtained over the same area and as a result both ambient magnetic field anomalies and magnetic gradients of the Earth's field were obtained at various stations. The minimum and maximum ambient field strength measurements observed over the study area are 31586.49 nT and 32733.46 nT with an average value of 32230.74 nT. Furthermore, the gradiometric values ranged from a minimum of −184.16 nT/m to a maximum of 152.35 nT/m. These two geophysical datasets comprising of the magnetic susceptibility and magnetic gradiometry datasets play complementary roles in defining the boundaries and the area extent of the waste deposit and their successes reported herein with their respective methods are attributed to the composition of ferrous metals within the waste. In this study, the methods to some extent, delineated potential leachate migration pathways, the boundaries and the area extent of the waste disposal site to be discussed later on in this chapter.

5.1.2 Digital Elevation Map of the Study Area

The area under study has an undulating topography and it is geologically underlain by precambian rocks of Birimian formation (figure 4.2). The highest elevated regions (B) and (A) are recorded at the central and eastern ends of the landfill with the lowest elevated region (D) recorded at the western and south–western ends of the landfill (figure 5.1). The region marked (B) is the main waste deposit with elevations varying from 291 m to 298 m above the mean sea–level and (A) is the immediate vicinity outside of the waste deposit.

In figure 5.1, region (A) by virtue of its high elevation causes the topography to dip towards the western and south–western directions. Again, due to the moderately low elevations towards the northern part of the waste disposal site with values ranging between 279 m and 289 m, the topography dips northwards as well. The sloping nature of the topography controls the hydrology of the area and as such, run–off water on the surface from rainwater, streams and groundwater follow this slope from areas marked (A) through to (D). This allows the creation of a model to image the areas of very low elevations (C and D) to have high risk of leachate flooding from the waste disposal site which is consistent with the work done by Bourgeois and Lavkulich (1972).

Consequently, the location of the SMA waste disposal site and the hydrology of the area do not favour settlements located close to the low lying areas (regions C and D of figure 5.1) as they stand high risk of leachate flooding due to their continuous dependence on groundwater. What is even more devastating is that these settlers farm and produce food crops on and around the waste body for public consumption.

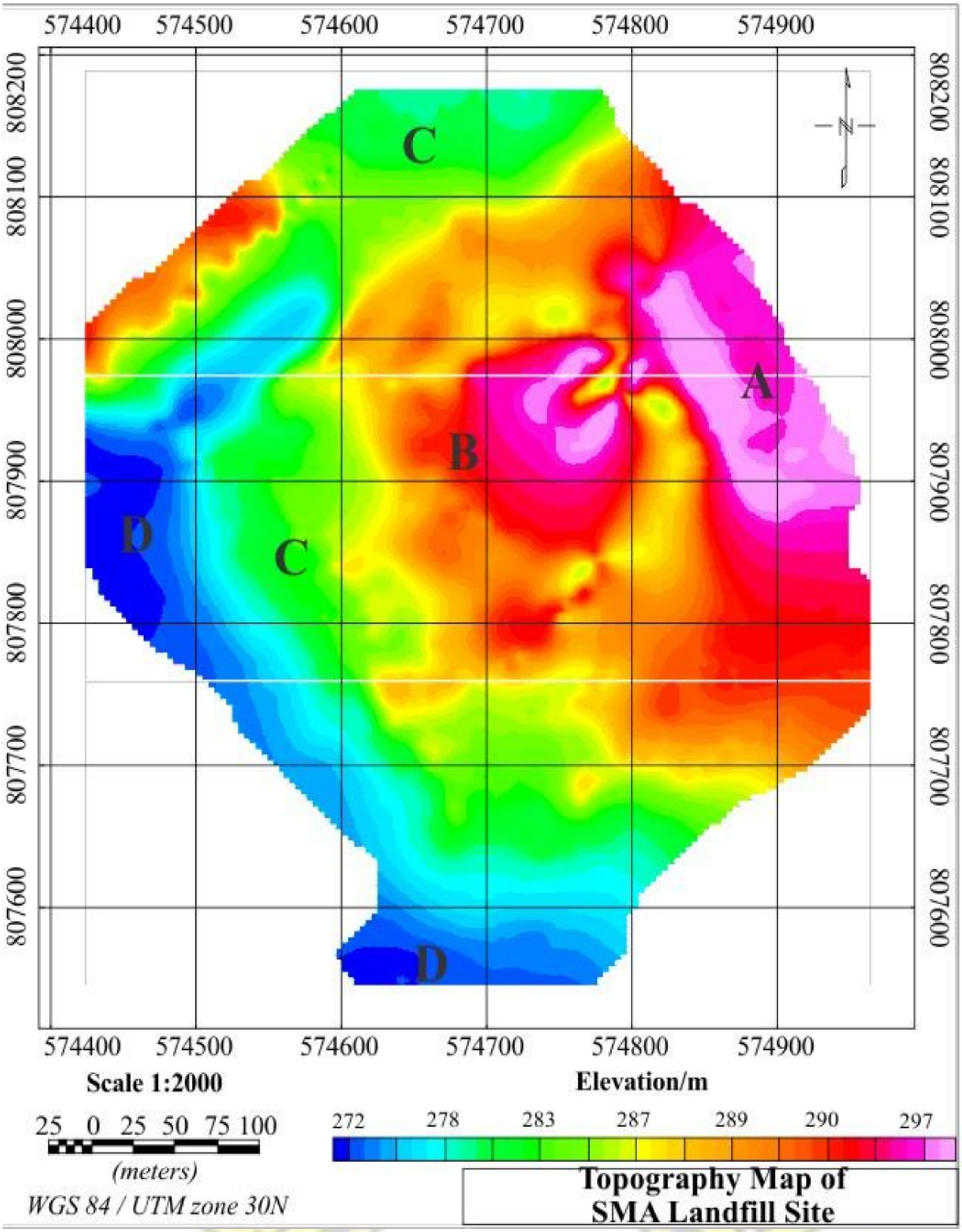

Figure 5.1: Digital Elevation Map of SMA Waste Disposal site near Asufofuo

5.1.3 Magnetic Susceptibility Model

The measurement of topsoil magnetic susceptibilities has been shown to be a very effective diagnostic tool in monitoring anthropogenic pollution in recent times for which reason it is used as proxies for rather expensive and laborious geochemical methods. This is based on the fact that soils with high magnetic susceptibilities tend to have high contents of ferro and ferrimagnetic minerals or elements. As part of the research objectives, the application of the magnetic susceptibility measurements sought to investigate the distribution of high magnetic susceptibility signatures of metalliferous materials which are major components of MSW, delineate the boundaries and the area extent of the waste deposit. To a large extent, the research also sought to determine the applicability of magnetic susceptibility measurements in delineating possible leachate contamination zones and preferential leachate migration pathways. This is made possible due to the fact that decomposing organic matter in the waste stream combines with rusting ferrous metals, ions and some heavy metals such as Mn, Fe, Cd, Co etc., in the presence of rainwater to provide a major sink for these pollutants in the ground. According to El Baghdadi et al. (2012), these heavy metals have high affinity to establish metallic bond with ferrous materials leading to enhancement in topsoil magnetic susceptibility as the leachate seeps into the ground from the landfill site. In effect, the high magnetic susceptibility signatures associated with both the landfill and leachate can be attributed to the high ferrous content of the waste driven by non separation of the waste.

The magnetic susceptibility distribution over the entire study area is shown in figure 5.2. Generally, three main zones of magnetic susceptibility signatures are identified. Regions A, B1, B2, B3 and B4 as shown in the figure 5.2 recorded the highest volume magnetic susceptibility values up to 9890×10^{-5} SI. Moderately high magnetic susceptibility signatures ranging between 100×10^{-5} SI and 2000×10^{-5} SI were also recorded over the entire study area. Relatively low magnetic susceptibility anomalies lower than 100×10^{-5} SI were also

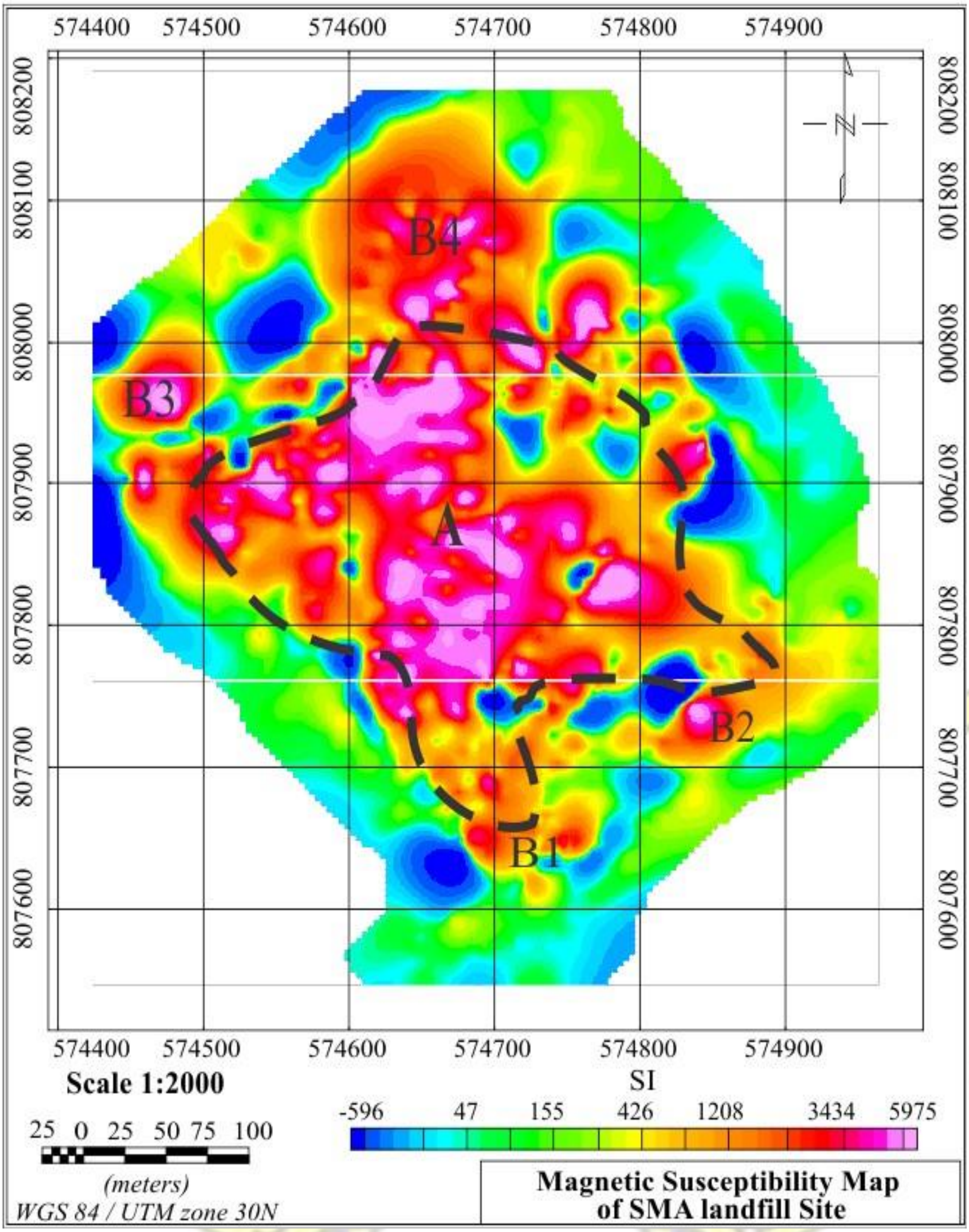

Figure 5.2: Magnetic Susceptibility Map of SMA Waste Disposal Site. The thick black dashed line shows the boundaries of the waste. B1, B2, B3 and B4 are regions of scattered waste from the main waste body.

identified. In all an average value of 1247.16×10^{-5} SI was observed with a standard deviation of 1981.24×10^{-5} SI. From the figure, it is noticeable that the main waste body (region A) is characterised by high magnetic signatures which delineated it from the background geologic materials. Region B4 recorded high magnetic susceptibility signatures outside the main boundary of the waste because of the huge piles of scrap metals gathered at that section by scavengers. Similarly, the anomalies recorded at regions B1, B2 and B3 are as a result of patches of waste outside the main delineated waste boundaries. On the whole, the results of the magnetic susceptibility measurements from figure 5.2 revealed that the mapped area extent of the main waste deposit is about 82,650 m^2.

5.1.4 Magnetic Gradiometry

Magnetometers have successfully been used to detect ferromagnetic and other metallic targets because they can measure the superposition of the geomagnetic field and the induced magnetic field in the targets depending on their volume magnetic susceptibilities (e.g., Marchetti et al., 2002; Marchetti and Settimi, 2011). On a whole, a total of 1,546 ambient field strength and gradiometric measurements were made during the entire period of the survey. Several magnetic gradient signatures ranging between −184.16 nT/m and 152.35 nT/m were recorded over the entire study area. Similarly, the ambient field anomalies were also measured and a range of values from a minimum of 31586.49 nT to a maximum of 32733.46 nT were obtained. An average value of 32230.74 nT was recorded over the area with values generally greater than the average measured over the main waste body.

Figure 5.3 shows the magnetic gradient anomaly map of the study area and because of the asymmetric nature of the magnetic data caused by the existence of remanent magnetisation direction, the amplitude of the magnetic gradient anomalies are displaced from their causative

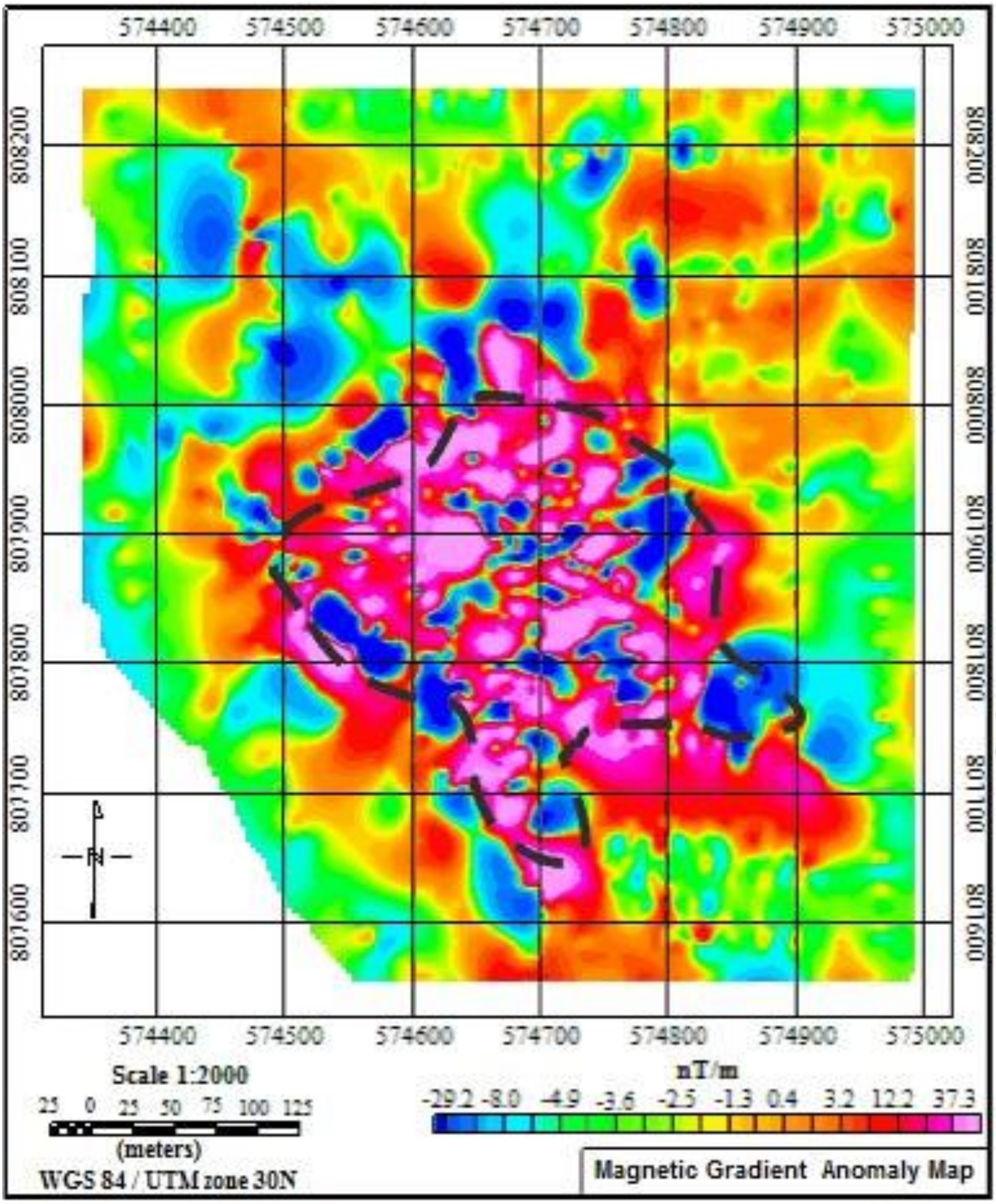

Figure 5.3: The Magnetic Gradient Anomaly Map without Analytic Signal Enhancement of the SMA Waste Disposal Site

sources. This can introduce errors in the interpretation of the magnetic data especially, when defining the exact location, geometry and boundary of the causative source are of the essence. Also, because the magnetic data was collected in Ghana which is just about 5^o N

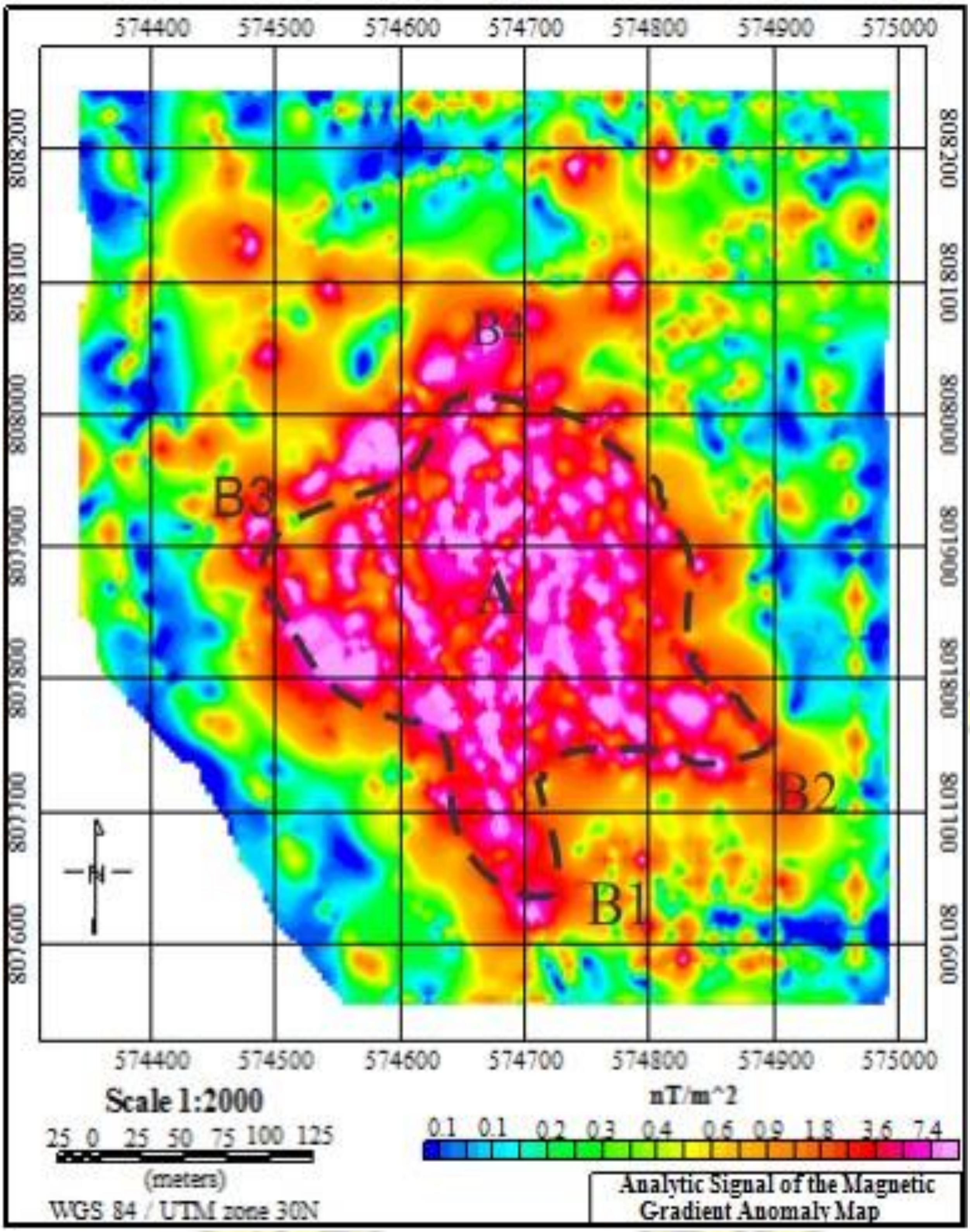

Figure 5.4: The Analytic Signal of the Magnetic Gradient Anomaly Map at the SMA Waste Disposal Site. The thick black dashed line shows the boundaries of the waste.

of the equator, the measured magnetic field intensity is smaller than high latitude magnetic data. This effect where areas of high magnetic susceptibility at low magnetic latitudes are depicted with low magnetic anomaly and vice versa is attributed to the influence of the geomagnetic field (Wemegah, 2015). This, coupled with shallow magnetic inclinations invariably obscure north–south striking magnetic and geological structures and renders them magnetically invisible. This phenomenon is clearly shown in figure 5.3 as areas of high magnetic susceptibilities are depicted with low magnetic signatures in comparison with 5.4.

Figure 5.4 shows the analytic signal of the magnetic gradient anomaly map of the study area indicating three main zones of magnetic signatures. The high magnetic signature at the central portion of the map, moderately high and low signatures erratically distributed around the main boundaries of the waste. In this figure, the main waste body is delineated with high magnetic anomalies due to the ferrous metal composition that discriminate it from the background geologic materials using the analytic signal operation. The analytic signal operation on the gradiometric data places the amplitude of the magnetic gradient anomalies directly above their causative sources to clearly define the boundaries of the waste at the SMA waste disposal site.

5.1.5 Electrical Resistivity Tomography Model

The ERT has shown to be very popular in both lateral and vertical delineation of wastes and leachate plumes in recent times (e.g., De Carlo et al., 2013; Lemke and Young, 1998). Due to the high content of organics, chloride, fluoride ions and other heavy metals in MSW composite, ground contamination from landfills are more electrically conductive than the surrounding formation containing small amount of contaminated pore water. For the fact that the electrical conductivity of a contaminated ground decreases with distance away from a contamination source under normal conditions, it is possible to adopt this phenomenon of ERT in characterisation of the MSW .

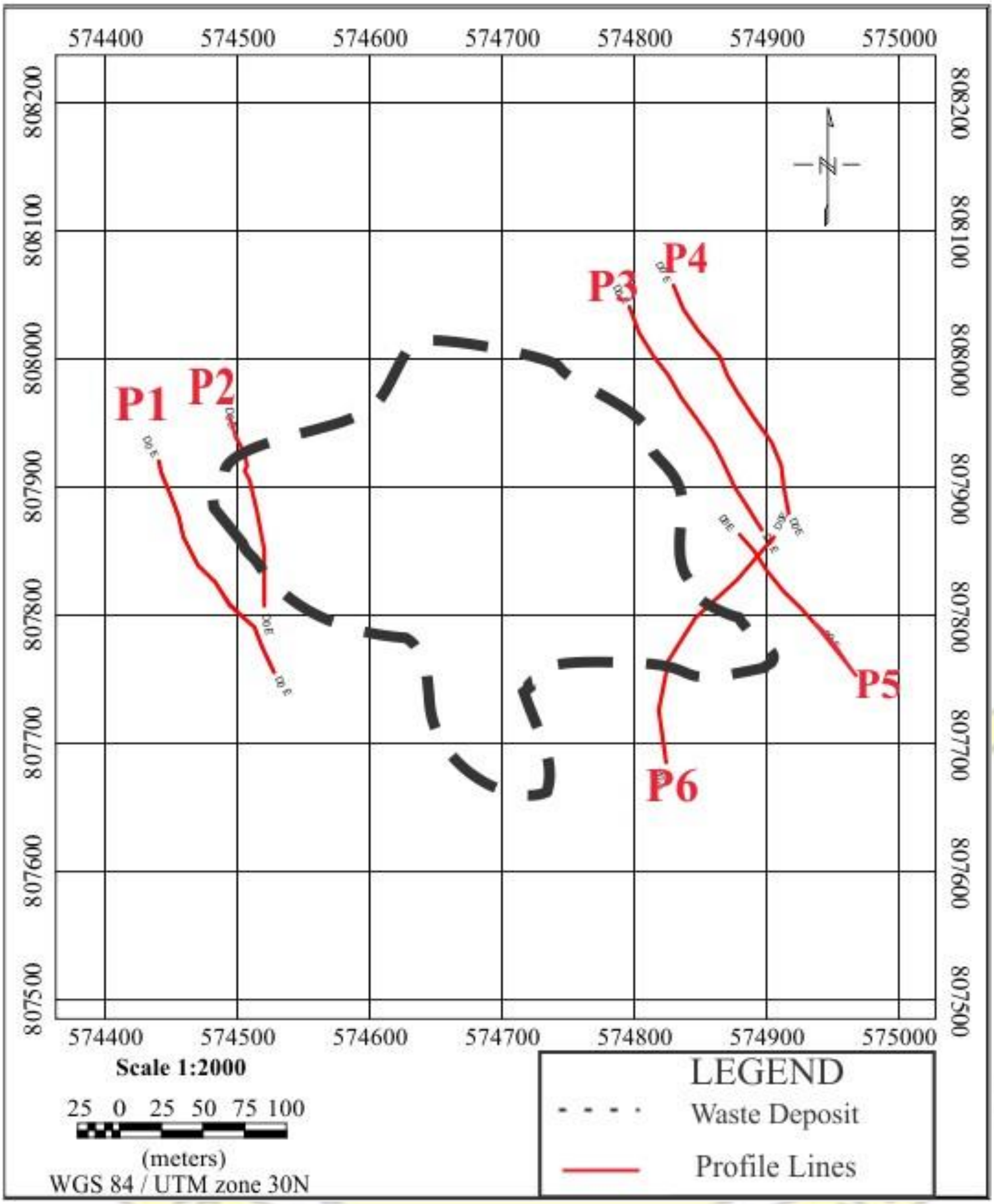

Figure 5.5: A Layout of the ERT Profiles at the SMA Waste Disposal Site

Figure 5.5 shows the layout of six profile lines on and around the immediate vicinity of the waste deposit. Profile one (P1) was selected at a distance of about 20 m from the western end of the main waste body to detect the possible presence of plumes due to leachate migration from the waste deposit. Profile two (P2) was selected to cut across the waste in order to compare the resistivity of the waste body, plume with the surroundings. Another reason was to determine the possibility of leachate infiltration into the ground directly beneath the waste deposit and the lateral extent of the plume. The profile line was laid about 38 m from north–western end of the waste body to pass across it through to about 130 m where the laid profile was made to move down the waste until a total profile length of 160 m was covered. Only two profile lines (P2 and P6) were laid across a small section on the waste body and the others were laid within the close vicinity of the waste. This was because the conditions at the site at the time the survey was conducted did not favour laying profiles on the waste. The major deterrent factor was burning of the waste which was exacerbated by the emission of smoke particles during the dry season. Respectively, profiles three and four (P3 and P4) were selected at a distance of about 15 and 30 m from the eastern part of the waste body. At the south–eastern end of the waste, profiles five and six (P5 and P6) were laid. P5 was laid perpendicular to the waste whereas P6 was laid at the side to monitor any possible migration of leachate from the site into those directions.

The results of the inversion of the six ERT profiles are displayed as cross–sections of the true resistivity distribution of the SMA waste disposal site. Figure 5.6a represents the resistivity section for P1 as shown in figure 5.5. It shows that the topography dips from the south towards the north at the western end of the waste disposal site. Unlike figure 5.6b, there is no clear distinction between any layers and the section is dominated by low resistivities between 10.0 $\Omega.m$ and 63.3 $\Omega.m$. Between these resistivity signatures, there is a gradual increasing trend in the directions indicated by the red arrows in figure 5.6a. However, 132 m to 166 m along the profile length, there is the existence of a relatively high resistive body of about 400 $\Omega.m$ between the elevations 235 m and 250 m.

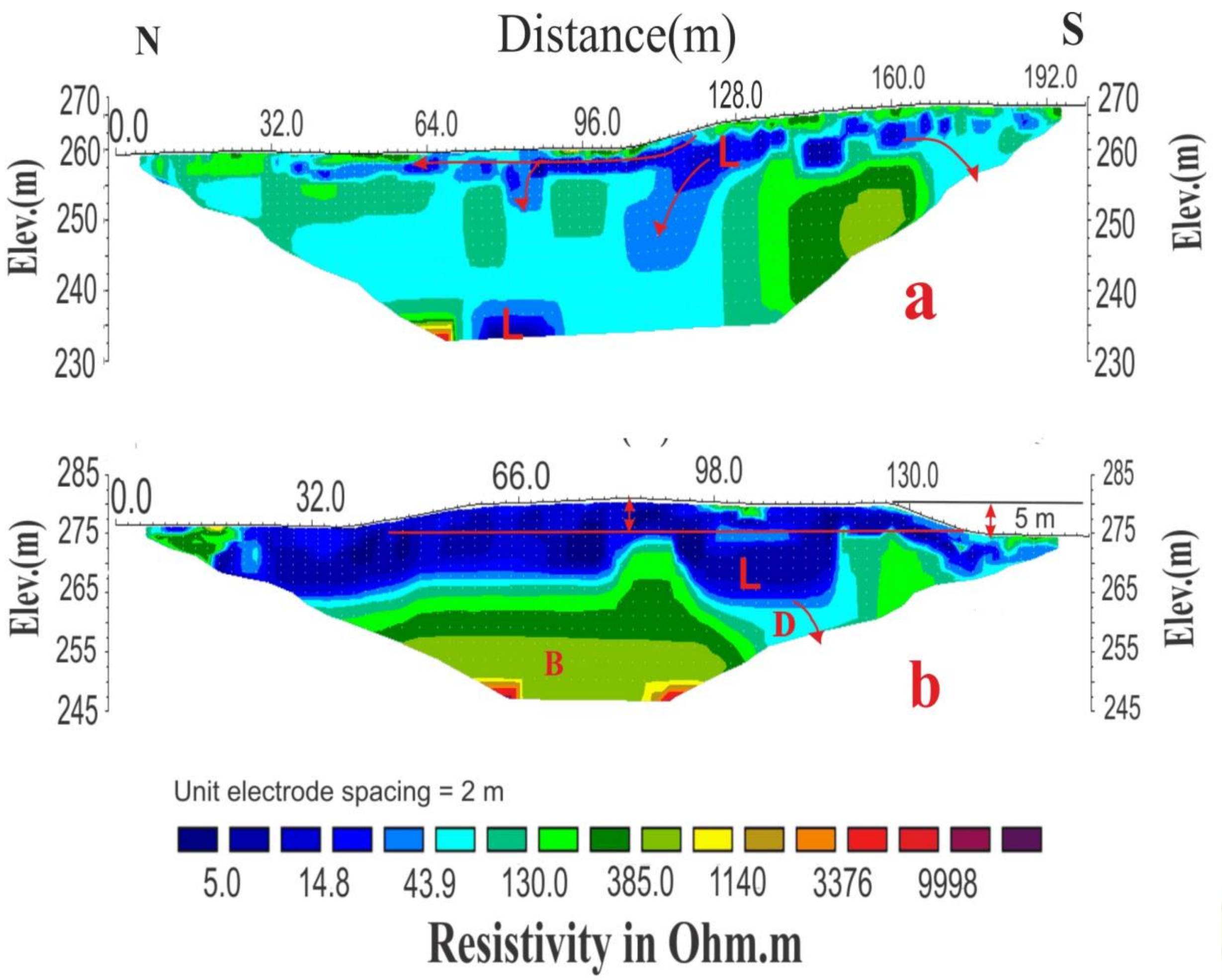

Figure 5.6: 2–D ERT Models at the Western Part of the Landfill. Red narrow line indicates the main waste average thickness, L representing zones of leachate accumulation while B represents bedrock beneath the topsoil surface and the red arrows indicating the preferential leachate migration pathways.

Figure 5.6b also represents the resistivity model section for P2 which shows two distinct zones of different electrical resistivity values. The top zone comprising of the main waste and leachate plumes has relatively very low electrical resistivities varying between 5.0 and 63 $\Omega.m$. The bottom zone (B) depicts gradual changes in resistivity signatures from a low of about 130 $\Omega.m$ to a high of over 6000 $\Omega.m$. This indicates a general upward trend in resistivity variations at deeper depths (lower elevations)

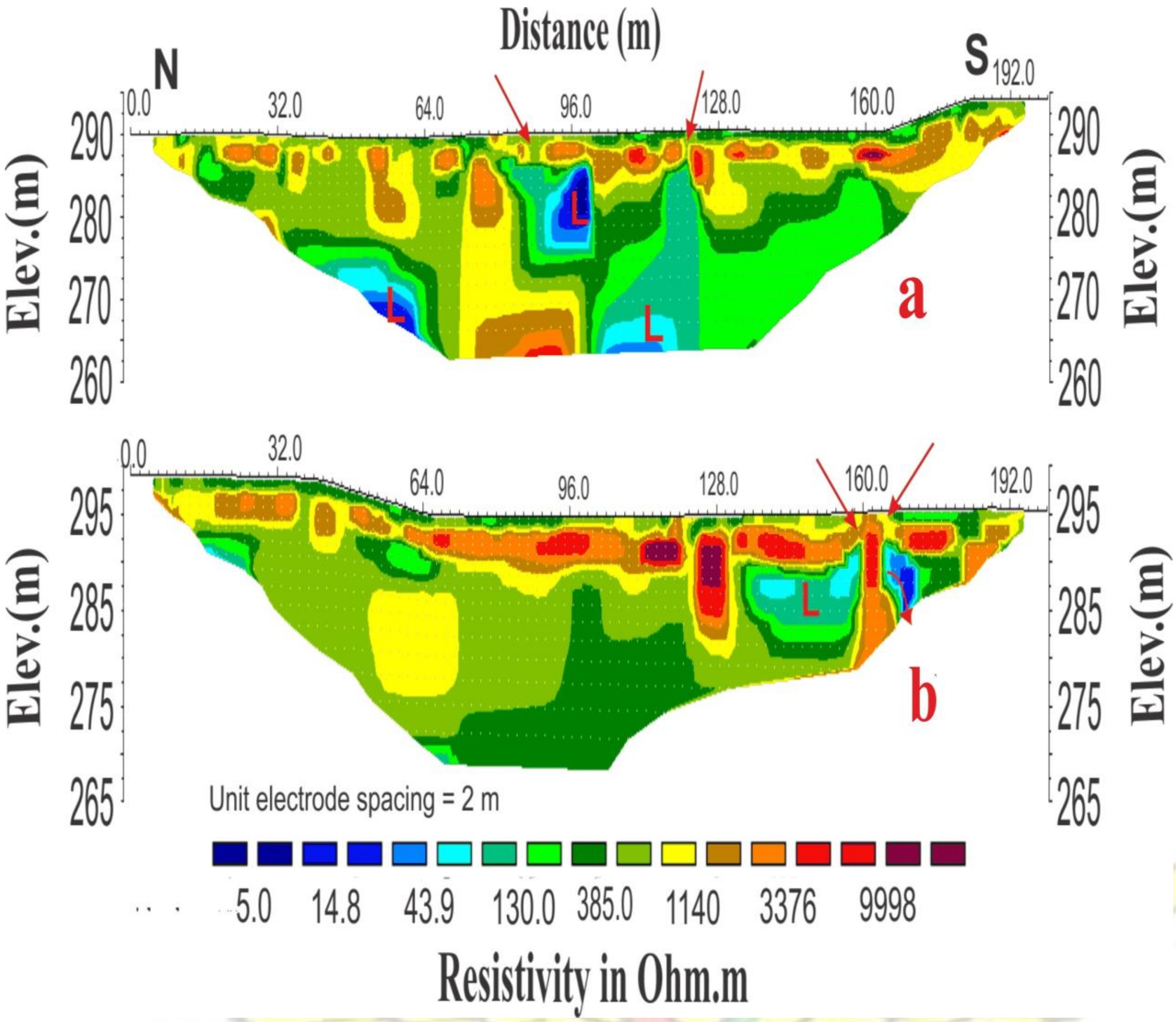

Figure 5.7: 2–D ERT Models at the Eastern Part of the Landfill. L representing zones of leachate accumulation and the top red arrows indicating pathways of leachate infiltration.

Figures 5.7a and 5.7b represent the 2–D ERT models for P3 and P4 as laid–out in figure 5.5 at the eastern end of the landfill where the elevation is highest. Both profiles depict higher electrical resistivity signatures at the top near–surface between 1140 $\Omega.m$ and 9998 $\Omega.m$ as compared with the relatively lower resistivity values at elevations lower than 280 m. One noticeable feature on the model for 5.7b is that the low resistive region between 130.0 m and 170 m along the profile line is split into two sections separated by a highly resistive material with the western section being more resistive than the eastern section. This could be due to the varying concentrations of leachate emanating from the waste with the western section having lower leachate concentrations.

Figures 5.8a and 5.8b also represent the 2–D ERT model sections for two profiles (P5 and P6) at the south–easting end of the landfill. Unlike figure 5.8b that was laid at the side of the waste, figure 5.8a was laid perpendicular to figure 5.8b away from the waste in order to observe the variations in electrical resistivity signatures in that direction. Figure 5.8a recorded relatively higher resistivity values greater than 385 Ω.*m* towards the areas with large distances from the landfill as a result of decreasing conductivity. Highly resistive materials of resistivities of about 3376 Ω.*m* were identified at few locations 5 m beneath the surface 30 m, 50 m and 80 m along the profile length.

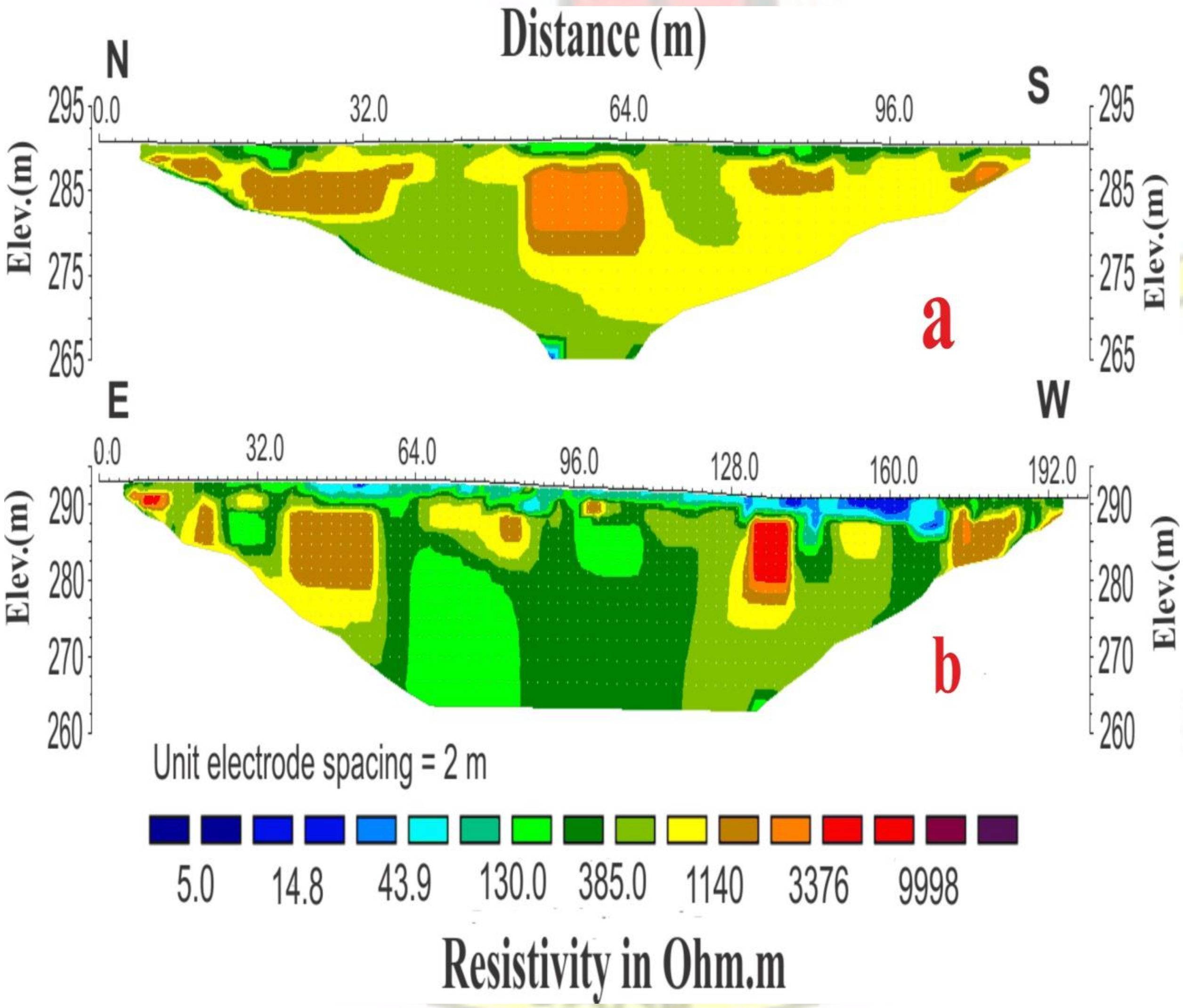

Figure 5.8: 2–D ERT Models at the Southern Part of the Landfill.

On the other hand, figure 5.8b was laid and passed across a small section of the waste with resistivity values generally lower than that of figure 5.8a because of the conductive nature of the ground that is influenced by high ionic content from the waste. At the immediate top surface of figure 5.8b, the resistivity signatures are lower ranging between 10 $\Omega.m$ and 70 $\Omega.m$. However, some locations were identified with high electrical resistivity signatures up to 3376 $\Omega.m$. These high anomalies were located at about 8 m beneath the surface at 44 m, 132 m and 176 m along the profile length.

5.2 Discussion

The magnetic susceptibility method having recorded an average magnetic susceptibility measurement of 1247.46×10^{-5} SI and a large standard deviation of 1987.24×10^{-5} SI, the data points are widely spread from the mean value. The large standard deviation obtained from the mean value can be attributed to the wide magnetic susceptibility contrast between the waste and background materials. Again, since most of the data points are centred at $0 - 1000 \times 10^{-5}$ SI class boundary, the probability plot of the data skews the curve to the right with a positive skewness of 2.25. This means that the right tail of the curve is longer relative to the left tail.

The results of the magnetic susceptibility survey have shown to be a sufficient mapping tool for characterising landfills. The measured high susceptibility signatures up to 9890×10^{-5} SI characterised the main waste body and delineated the boundaries of the waste deposit (region A). The magnetic susceptibility survey clearly outlined the geometry of the main waste body with an approximate area of 82,650 m^2. This was only feasible due to the large ferrous metal content in the waste stream. The results of both magnetic susceptibility and gradiometric methods give an indication that municipal solid waste management which encompasses major components such as source separation, recovery and recycling are not practised in the municipality. Also, the high anomalies recorded outside the designated boundaries of the main waste body (regions B1, B2 and B3) are clear indications of indiscriminate deposition of SW in the area based on previous studies by Wemegah et al. (2014). The general magnetic susceptibility signature around the waste tends to decrease with increasing distance from the waste. These areas recorded most of the lowest susceptibility values ranging between about 1.0×10^{-5} SI to 50×10^{-5} SI which is largely indicated by the blue and light blues colours in figure 5.2. The measured susceptibilities compared with the susceptibilities of materials measured by Dearing (1999) and Boadi et al. (2014) suggest the likely presence of paramagnetic and canted antiferromagnetic minerals because the observed magnetic susceptibility readings are relatively small and positive.

In a similar development, statistical analysis of the gradiometric data revealed that the average value of the magnetic gradient of the Earth's field obtained over the entire study area was 3.45 nT/m with a standard deviation of 28.76 nT/m. Again, comparing the mean value with the large standard deviation, there is a large spread out of the data over a wide range of values. The significance of this is that there is sufficiently high magnetic susceptibility contrast over the area which delineated the waste. With a skewness as low as 0.013, the probability plot of the data slightly skews the curve to the right.

The results obtained by using the gradiometric method is not different from that obtained by the magnetic susceptibility measurements as far as the geometry (lateral extent) of the waste is concerned. In both figures (i.e, 5.2 and 5.4), the physical property contrast between the waste composite and the surrounding geology for both methods clearly delineates the boundaries and the area extent of the waste at the waste disposal site. The low magnetic susceptibility signatures indicated within the delineated waste boundary in figure 5.2 is attributed to the fact that the MS2D loop sensor could only probe to a depth of about 100 cm and did not therefore detect sources of high anomalies buried deep inside the waste. Comparing with figure 5.4 indeed revealed high anomalous sources in those regions using the gradiometer. This is because the passive gradiometric method could probe deeper to detect buried metalliferous materials inside the waste. The irregular nature of the distribution of magnetic signatures can be ascribed to the inhomogeneity in the distribution of metalliferous materials in the waste deposit. On the basis of previous geophysical investigations on landfills (e.g., Wemegah et al., 2014), the high magnetic anomalies outside the boundaries of the main waste deposit is as a result of indiscriminate deposition of waste over the entire study area.

The results of the 2–D ERT models show that electrical resistivity method is useful for characterising the distribution of certain materials in MSW, soil and groundwater. This is evident in figure 5.6b due to the sharp resistivity contrast within the section. The electrical resistivity section depicts a clear distinction between two layers, the top layer with elevations ranging between 280 m and 265 m and the bottom layer. From this figure, the top layer of resistivities lower than 43.9 $\Omega.m$ characterised the waste body and the background topsoil saturated with leachate just beneath the waste. With reference to other landfill studies, (e.g., Shemang et al., 2011; Abdullahi et al., 2011), low resistivity signatures may result from increase in ion load by leachate emanating from the waste. The red horizontal line is the interface the separates the waste bottom from the background topsoil. In the top layer, the part above the red line as shown in figure 5.6b is attributable to the main waste body and beneath it is the background topsoil saturated with leachate. From figure 5.6b, it is evident that the resistivity of the leachate contaminated topsoil beneath the waste is apparently indistinguishable from the bottom of the main waste deposit because there is no sufficient resistivity contrast between them due to their overlapping low resistivities causes by the infiltration of the leachate from the waste. The estimation of the thickness of the waste body from the model section was therefore difficult to deduce on the basis of only the electrical signatures of the waste and the leachate plume. This occurrence renders the electrical resistivity method less effective in estimating the thickness of waste deposits with greater precision in unlined waste disposal sites. However, when the data was corrected to allow the topography of the surface the thickness of the waste at the western section was estimated to be 5 m. The approximate thickness of the waste is obtained by computing the difference in the elevations between the top of the waste and the immediate level ground.

In another development, region (B) at the bottom layer of figure 5.6b with relatively high electrical resistivity values is interpreted to represent the weathered part of the bedrock material beneath the waste deposit. The increasing trend in horizontal electrical resistivity variations is an indication that the weathered part of the bedrock with varying degree of compaction has not been penetrated with leachate from 36 m to 98 m along the profile despite the absence of landfill liner. However, from about 110 m to 120 m along the profile line (region D of figure 5.6b), the accumulation of leachate is interpreted to be a path for leachate infiltration and migration due to the horizontal changes in the resistivity signatures.

Figure 5.6a gives indications of contaminated zones of saturation just some few meters beneath the top surface with resistivity range of about 15 $\Omega.m$ to 50 $\Omega.m$. The low resistivity signatures just beneath the ground surface could be attributed to zones of high leachate activity. Since leachate is highly conductive, it produces very low resistivity signatures and the lowest where it mostly accumulates as well as its contaminant sources. Similar results were obtained by Abdullahi et al. (2011) who represented the resistivity of the contaminated zones of saturation with lower signature ranging between 15.3 $\Omega.m$ and 40.5 $\Omega.m$. A cursory look at the resistivity section of figure 5.6a suggests that the topography dips from the south towards the northern direction and that both surface run–off and polluted groundwater with varying concentrations of contaminants from the waste deposit follow the hydraulic gradient of that section of the profile. As the contamination plume moves, it spreads both laterally and vertically away from the main source of contamination towards the direction of water movement. From the figure, it spreads from the site of highest concentration of contaminants towards the site of lowest concentration. This is evident with the gradual increase in resistivity signatures from the low anomalous zones along the directional arrows as shown in figure 5.6a which depicts a gradual transition from deep blue to light blue on the colour scaling. This is occasioned by the variations in concentrations of the plume as it spreads laterally and vertically through the ground. The lateral and vertical directional arrows indicate the preferential migration pathways of the leachate plume from the source of concentration (L) in the figure above.

On the other hand, the profiles at the eastern perimeter (figure 5.7) have relatively higher resistivity signatures from about 5 m below the top surface. The high resistivity values greater than 1140 $\Omega.m$ and located below 5 m of the top surface can be attributed to the likely presence of dense duricrusts that block the percolation of leachate through that part of the ground. This is based on previous studies conducted by Hill (2003) close to the study area. Notwithstanding the likely presence of the highly resistive duricrusts, some areas characterised by low resistivity range between 5.0 $\Omega.m$ and 43.9 $\Omega.m$ were detected at greater depths which are interpreted to be zones of leachate accumulation. These zone were detected at about 56.0 m, 96.0 m and 110.0 m along the surface at various depths as depicted in figure 5.7a. It is believed that the leachate may have seeped through the ground along paths indicated by the red arrows. The study area consisting of a resistive layer of saprolites underlie the duricrusts (Hill, 2003) and so confine the leachate plumes to specific locations as shown in figure 5.7a. Similar phenomenon occurs with figure 5.7b at 160 m along the survey line but the contamination extent is minimised. This can be attributed to the fact that figure 5.7b is far away from waste deposit relative to figure 5.7a and the highest elevation at the eastern end of the landfill may have also contributed to the lower leachate content.

The results of inversion of the two ERT profiles, P5 and P6 at the south–easting perimeter of the waste showed no indication of low resistivity signatures (contamination plumes) as indicated in figure 5.8. The apparent increase in resistivity along figure 5.8a suggests the absence of fluid migration pathways due to the high elevation that characterises that part of the waste disposal site. Figure 5.8b which was laid to cut across a small section and closer to that side of the main waste deposit has relatively lower resistivity signatures especially at the top surface. This may have been influenced by the relative location of the profile line having greater ionic content. The very low resistivity signatures at the top surface of the profile line is attributable to the small section of waste that was cut across during the survey. Other sources of the very low resistivity signatures at the top surface of the profile line is attributed to the initial assertion of indiscriminate disposal of the solid waste especially, at the south–eastern part of the waste disposal site.

The results of the research indicate that the location of the waste deposit has dire repercussions on the environment and the settlers surrounding it and therefore, the continuous usage of the area as a waste disposal site should be discouraged. This is due to the presence of delineated plume patterns within the ground and what is more, is the proximity of the water table to the ground surface at the western perimeter of the waste deposit. From the results of both magnetic susceptibility and gradiometric methods, the geometry of the main waste body (region A of figures 5.2 and 5.4) is delineated with high magnetic signatures covering averagely, an area of of about 82,650 m^2. With an average thickness of about 5 m, the volume of waste at the SMA waste disposal site is estimated to be 413,250 m^3.

Chapter 6

CONCLUSIONS AND RECOMMENDATIONS

6.1 Conclusions

In conclusion, the applications of three integrated geophysical methods involving the electrical resistivity tomography, magnetic susceptibility and magnetic gradiometry methods in the characterisation of the SMA waste disposal site have successfully met the objectives. The study involved the deployment of geophysical equipment comprising of the ABEM SAS 4000 terrameter, magnetic susceptibility meter and MS-2D Bartington loop sensor and the gradiometer on different areas in and around the Sunyani waste disposal site. The data acquired by these equipment aided in deriving useful depth and horizontal information about the thickness of the waste, presence and extent of incursions of contamination plumes and finally preferential pathways of leachate plumes for the purpose of remediations and

regulations.

In landfill studies, the electrical properties are largely influenced by factors such as, age of landfill, porosity of the background geology, ionic concentration and moisture content in the waste deposit. The latter was controlled to some extent as the study was conducted in the dry season (month of December) in order to obtain a 'true resistivity distribution'of the subsurface. At the western end of the waste site where the bulk of the waste was deposited, the ERT model clearly delineated the waste and leachate plume from the weathered bedrock due to greater resistivity contrast between the waste body and the weathered bedrock. From the analysis of the data, the average thickness of the waste body at the western part is estimated to be 5.0 m from the ERT model in profile two of figure 5.6. This estimated thickness of the waste deposit from the model section was difficult to deduce on the basis of only electrical resistivity signatures due to the clear overlap between the signatures produced from both waste and leachate. As a result, the difference in elevations from the top of the waste body and the bottom ground level from the model resistivity section was used to obtain an approximate waste thickness of 5.0 m. Therefore, the application of ERT in determining with greater accuracy, the thickness of solid waste deposits in unlined landfills is not very effective because of the potential for leachate infiltration with low resistivity range comparable to the waste body. Though, not very effective in estimating the thickness of the waste, the ERT clearly delineated low resistive zones which are attributed to leachate migration pathways within the study area and it follows that the direction of the leachate flow is towards that of the groundwater movement (east–west and south–western directions) due the high topographic gradient in those directions. The presence, horizontal and vertical extent of contamination plumes were delineated by the geo–electrical method as a consequence of varying electrical resistivity in the contaminated area.

Both magnetic susceptibility and gradiometric measurements clearly delineated the boundaries of the waste deposit with an approximate area of 82,650 m^2. From figure 5.2, four distinct regions of varying magnetic susceptibilities were identified. The region (A) with the highest susceptibility record defined the boundaries of the waste. This was possible as there was substantially high magnetic susceptibility contrast between the waste and its surrounding geologic materials due to the high content of ferrous metals in the waste. The second regions (B1, B2, B3 and B4) also represent high anomalous zones resulting from scattered waste and separated scrap metals from the main waste body. The third and fourth regions identified by light–green and deep blue colours of figure 5.2 characterised low leachate contaminated and paramagnetic sediments.

The integration of electrical resistivity, magnetic susceptibility and gradiometric methods in measuring different physical properties of the subsurface have aided in the characterisation of the SMA waste disposal site successfully. The main purpose of integrating these methods is to minimise ambiguities in interpretation associated with a single method. The study has also revealed that the electrical resistivity and magnetic susceptibility and gradiometric methods are very effective in landfill studies.

6.2 Recommendations

The fundamental limitation of the lack of sufficient electrical resistivity contrast to clearly discriminate solid waste deposits from leachate plumes presents an enormous challenge to environmental geophysicists in estimating with greater precision the thickness of waste deposits. In view of the results and depth information acquired from this research, the electrical resistivity method was not a very effective method in determining the thickness of waste at the SMA waste disposal site. It is therefore recommended that time–domain spectral induced polarisation and self–potential measurements should be deployed at the site in order to complement the results obtained by the ERT method.

Boreholes must be drilled to greater depths to replace the hand–dug wells for the settlements at the western part of the waste site. This is because the depth to the water level is few meters beneath the surface for two monitored hand–dug wells. The preferred region for drilling boreholes is the south–eastern part of the waste disposal site since there were no indications of leachate contamination.

Also, the waste disposal site ought to be engineered to underlie the waste body with a protective liner such as HDPE plastics or clay to prevent the poisonous contaminants from the waste from infiltrating into the ground to pollute the groundwater. These materials are highly recommended because they have been known to be impermeable to migrating fluids and therefore confine them to only the waste.

Finally, there is the need for waste managers to consider bioremediation since certain bacteria have the capability of degrading a variety of organic pollutants that are persistently present in leachate to reduce the toxicity of the leachate that pollutes the groundwater.

References

Abd El–Salam, M. M. and Abu-Zuid, G. I. (2015). Impact of landfill on the groundwater quality: A case study in egypt. *Journal of Advanced Research*, 6:579–586.

Abdullahi, N. K., Osazuwa, I. B., and Sule, P. O. (2011). Application of integrated geophysical techniques in the investigation of groundwater contamination: A case study of municipal solid waste leachate. *Ozean Journal of Applied Sciences*, 4(1).

ABEM Instrument AB (2008). *Abem instruction manual*. ABEM Printed Matter No 93109.

Abu-Rukah, Y. and Al-kofahi, O. (2001). The assessment of the effect of landfill leachate on ground-water quality: a case study. el-akader landfill site-north jordan. *Journal of Arid Environments*, 49:615–630.

Al-Yaqout, A. F. and Hamoda, M. F. (2003). Evaluation of landfill leachate in arid climate–a case study. *Environment international*, 29(5):593–600.

Aning, A. A., Tucholka, P., and Danuor, S. K. (2013). 2d electrical resistivity tomography (ert) survey using the multi-electrode gradient array at the bosumtwi impact crater, ghana. *Journal of Environment and Earth Science*, 3(5):12–27.

Belghazal, H., Piga, C., El Messari, J. S., and Touhami, A. O. (2013). Geophysical surveys for the characterization of landfills. *International Journal of Innovation and Applied Studies*, 4(2):254–263.

Bernstone, C. and Dahlin, T. (1997). dc resistivity mapping of old landfills: Two case studies. *European Journal of Environmental and Engineering Geophysics*, 2:121–136.

Boadi, B., Preko, K., and Amekudzi, L. K. (2014). Implications of soil magnetic susceptibility measurements from the waste site deposit of independence hall, kwame nkrumah university of science and technology (knust), kumasi. *International Journal of Scientific and Research Publications*, 4(5):1–7.

Boateng, E., Asare, V. S., and Danour, S. K. (2013). Detection and delineation of contaminant migration using the terrain conductivity technique outside the perimeters of the dompoase landfill facility in kumasi–ghana. *Journal of Environmental and Earth Science*, 3(2):13–14.

Bourgeois, W. W. and Lavkulich, L. M. (1972). A study of forest soils and leachates on sloping topography using a tension lysimeter. *Canadian Journal of Soil Science*, 52(3):375–391.

Carlson, N. R., Hare, J. L., and Zonge, K. L. (2001). Buried landfill delineation with induced polarization: Progress and problems. *In Proceedings of the 2001 Symposium on the Application of Geophysics to Engineering and Environmental Problems (SAGEEP). Denver, Colorado, March 4–7, 2001*.

Cochran, J. R. and Dalton, K. E. (1995). Using high-density magnetic and electromagnetic data for waste characterization, a case study. *In Proceedings of the Symposium on the Application of Geophysics to Engineering and Environmental Problems, edited by R. S. Bell. Environmental and Engineering Geophysical Society, Orlando, Florida*, page 117.

Cudjoe, J. E. (1961). A programme for geophysical exploration in ghana. Master's thesis, Massachusetts Institute of Technology, Massachusetts, US.

Dahlin, T. (2012). Application of resistivity-ip to mapping of groundwater contamination and burried waste. *Geophysical Association of Ireland Seminar on Environmental Geophysics Dublin, 15th February 2012*.

Dahlin, T., Rosqvist, H., and Leroux, V. (2010). Resistivity-ip mapping for landfill applications. *First Break*, 28(8):101–105.

Dahlin, T. and Zhou, B. (2006). Multiple-gradient array measurements for multichannel 2d resistivity imaging. *Near Surface Geophysics*, 4(2):113–123.

De Carlo, L., Perri, M. T., Caputo, M. C., Deiana, R., Vurro, M., and Cassiani, G. (2013). Characterization of a dismissed landfill via electrical resistivity tomography and mise-la-masse method. *Journal of Applied Geophysics*, pages 1–10.

Dearing, J. A. (1999). *Environmental Magnetic Susceptibility: Using the Bartington MS2 System*. Chi publishing, England, 2nd edition.

Denutsui, D., Akiti, T. T., Osae, S., Tutu, A. O., Blankson-Arthur, S., Ayivor, J. E., Adu-kwame, F. N., and Egbi, C. (2012). Leachate characterization and assessment of unsaturated zone pollution near municipal solid waste landfill site at oblogo accra-ghana. *Research Journal of Environmental and Earth Sciences*, 4(1):134–141.

El Baghdadi, M., Barakat, A., Sajieddine, M., and Nadem, S. (2012). Heavy metal pollution and soil magnetic susceptibility in urban soil of beni mellal city (morocco). *Journal of Environmental and Earth Science*, 66(1):141–155.

ESP (1999). Government of ghana, ministry of local government and rural development. environmental sanitation policy. http://www.mlgrd.gov.gh/files/file/download/ 330/?next=/library/documents/. Accessed on: March 26, 2016.

ESP (2010). Government of ghana, ministry of local government and rural development. environmental sanitation policy, (revised 2010),. http://www. ecowrex.org/system/files/repository/2010_environmental-sanitation-policy_ ministry-of-local-government-and-rural-development.pdf. Accessed on: July 19, 2016.

Fadhli, Z., Saad, R., Nordiana, M. M., Azwin, N., and Bery, A. A. (2015). Mapping subsurface karst formation using 2-d electrical resistivity imaging. *Electronic Journal for Geotechnical Engineering*, 20.

Furness, P. (2007). Modelling magnetic fields due to steel drum accumulation. *Geophys. Prospect.*, 55(5):737–748.

Gazoty, A., Fiandaca, G., Pederson, J., Auken, E., and Christiansen, A. V. (2012). Mapping of landfills using time–domain spectral induced polarization data: The eskelund case study. *Near Surface Geophysics*, 10:575–586 doi:10.3997/1873–0604.2012046.

Gilkeson, R. H., Gorin, S. R., Weston, R. F., and Laymon, D. E. (1992). Application of magnetic and electromagnetic methods to metal detection. *In Proceedings of the Symposium on the Application of Geophysics to Engineering and Environmental Problems April 26-29, 1992, Oakbrook, Illinois*, pages 309–328.

Grant, F. S. and Dodds, J. (1972). *MAGMAP FFT processing system development notes*. Paterson Grant and Watson Limited.

GSS (2014). District analytical report, sunyani municipality, ghana statistical service (gss). www.statsghana.gov.gh/docfiles/2010_District_Report/.../Sunyani%20Municipal.pdf. Accessed on: July 20, 2016.

Hanesch, M. and Scholger, R. (2002). Mapping of heavy metal loadings in soils by means of magnetic susceptibility measurements. *Environ Geol*, 42:857–870.

Hill, R. (2003). Ahafo project feasibility study. Technical report, Newmont Ghana Gold Ltd.

Hoornweg, D., Bhada-Tata, P., and Kennedy, C. (2013). Environment: Waste production must peak this century. *International weekly journal of science*, 502:615–617.

Jhamnani, B. and Singh, S. K. (2009). Groundwater contamination due to bhalaswa landfill site in new delhi. *Int. J. Environ. Sci. Eng*, 1(3):121–125.

Junner, N. R. (1935). Gold in the gold coast. *Ghana Geol. Surv. Mem.*, (464p).

Karimi, R., Ayoubi, S., Jalalian, A., Sheikh-Hosseini, A. R., and Afyuni, M. (2011). Relationships between magnetic susceptibility and heavy metals in urban topsoils in the arid region of isfahan, central iran. *Journal of Applied Geophysics*, 74:1–7.

Kearey, P. and Brooks, M. (1991). *An Introduction to Geophysical Exploration*. Blackwell Science, Oxford, 2nd edition.

Kearey, P., Brooks, M., and Hill, I. (2002). *An Introduction to Geophysical Exploration*. Blackwell Science, Osney Mead, Oxford OX2 0EL, 3rd edition.

Kesse, G. O. (1985). *The Mineral and Rock Resources of Ghana*. Rotterdam, A. A. Balkema.

Khanal, S. A. (2007). Post project environmental monitoring and impact assessment - a case study of gokarna landfill site after operation and closure. *Scientific World*, 5(5):60–66.

Le Borgne, E. (1955). Susceptiblit´e magn´etique anormale du sol superficiel. *Ann. G´eophys*, 11:399–419.

Lecoanet, H., L´evˆeque, F., and Segura, S. (1999). Magnetic susceptibility in environmental applications: comparison of field probes. *Physics of the Earth and Planetary Interiors*, 115:191–204.

Lemke, S. R. and Young, C. T. (1998). Leachate plume investigations using mise-a-la-masse resistivity. *Proceedings of the Symposium on the Application of Geophysics to Engineering and Environmental Problems*, pages 839–847.

Leube, A., Hirdes, W., Mauer, R., and Kesse, G. O. (1990). The early proterozoic birimian supergroup of ghana and some aspects of its associated gold mineralization. *Precambrian Research*, 46:139–165.

Loke, M. H. (2000). *Electrical imaging surveys for environmental and engineering studies: A practical guide to 2–D and 3–D surveys*. Georentals, UK.

Macleod, I. N., Jones, K., and Dai, T. F. (1993). 3–d analytic signal in the interpretation of total magnetic field data at low magnetic latitude. *Exploration Geophysics*, 24:679–688.

Mantlik, F., Matias, M., Louren¸co, J., Grangeia, C., and Tareco, H. (2009). The use of gravity method in the internal characterization of landfills–a case study. *Journal of Geophysics and Engineering*, 6(4):357–367.

Marchetti, M., Cafarella, L., Di Mauro, D., and Zirizzotti, A. (2002). Ground magnetometric survey and integrated geophysical methods for solid buried waste detection: a case study,. *Annals of Geophysics*, 45(3–4):563–573.

Marchetti, M. and Settimi, A. (2011). Integrated geophysical measurements on a test site for detection of buried steel drums. *ANNALS OF GEOPHYSICS*, 54(1):105–114, doi: 10.4401/ag–4846.

Miezah, K., Obiri-Danso, K., Ka´d´ar, Z., Fei-Baffoe, B., and Mensah, M. Y. (2015). Municipal solid waste characterization and quantification as a measure towards effective waste management in ghana. *Waste Management*, http://dx.doi.org/10.1016/j.wasman.2015.09.009.

Milesi, J. P., Feybesse, J. L., Dommanget, A., Ouedraogo, M. F., Marcoux, E., and Prost, A. (1990). West african gold deposits in their lower proterozoic lithostructural seeting. *Chron. Rech. Min*, 497:3–98.

Milsom, J. (2003). *Field Geophysics: The Geological Field Guide Series*. John Wiley and Sons Ltd, The Atrium, Southern Gate, Chichester, West Sussex PO19 8SQ, England, 3rd edition.

Moreno-Sanchez, R. D. and Maldonado, J. H. (2006). Surviving from garbage: the role of informal wastepickers in a dynamic model of solidwaste management in developing countries. *Environment and Development Economics*, 11:371–391.

Mullins, C. E. (1977). Magnetic susceptibility of the soil and its significance in soil science a review. *J. Soil Sci.*, 28:223–246.

Nabighian, M. N. (1972). The analytic signal of two–dimensional magnetic bodies with polygonal cross–section: Its properties and use for automated anomaly interpretation. *Geophysics*, 37(3):507–517.

Nagabooshnam, J. K. (2011). Solid waste generation and composition in gaborone, botswana, potential for resource recovery. Master's thesis, Energy and environmental engineering, Department of Management Engineering, Linkoping University, Sweden.

Osei-Mensah, P., Adjaottor, A. A., and Owusu-Boateng, G. (2014). Characterization of solid waste in the atwima–nwabiagya district of the ashanti region, kumasi–ghana. *International Journal of Waste Management and Technology*, 2(1):1–14.

Owusu, D. K. (2010). *Waste management projections*. Environmental Health Department, Sunyani Municipal Assembly.

Palacky, G. J. (1988). Resistivity characteristics of geologic targets. *Society of Exploration. Geophysics*, pages 52–129.

Petrovsky, E., Kapicka, A., Jordanova, N., Knab, M., and Hoffmann, V. (2000). Low-field magnetic susceptibility: a proxy method of estimating increased pollution of different environmental systems. *Environmental Geology*, 39:312–318.

Porsani, J. L., Filho, W. M., Elis, V. R., Shimeles, F., Dourado, J. C., and Moura, H. P. (2004). The use of gpr and ves in delineating a contamination plume in a landfill site: a case study in se brazil. *Journal of Applied Geophysics*, 55:199–209.

Roest, W. R., Verhoef, J., and Pilkington, M. (1992). Magnetic interpretation using 3–d analytic signal. *Geophysics*, 57(1):116–125.

Schmidt, A., Yarnold, R., Hill, M., and Ashmore, M. (2005). Magnetic susceptibility as proxy for heavy metal pollution: a site study. *Journal of Geochemical Exploration*, 85:109–117.

Shemang, E. M., Mickus, K., and Same, M. P. (2011). Geophysical characterization of the abandoned gaborone landfill, botswana: Implications for abandoned landfills in arid environments. *International Journal of Environmental Protection*, 1(1):1–12.

Singer, M. J., Verosub, K. L., and Fine, P. (1996). A conceptual model for the enhancement of magnetic susceptibility of soils. *Quatern. Int.*, pages 34–36,243–248.

SMA (2010). Physical characteristics, ministry of local government and rural development (mlgrd). http://www.ghanadistricts.com/DistrictSublinks.aspx?s=4283&d=50. Accessed on: July 21, 2016.

Strzyszcz, Z. and Magiera, T. (1998). Magnetic susceptibility and heavy metals contamination in soils of southern poland. *Phys. Chem. Earth*, 23(9–10):1127–1131.

Telford, W. M., Geldart, L. P., and Sheriff, R. E. (1990). *Applied Geophysics*. Cambridge University Press, The Pitt Building, Trumpington Street, Cambridge CB2 1RP, 2nd edition.

Thompson, R. and Oldfield, F. (1986). *Environmental Magnetism*. Allen and Unwin, London.

UNEP (2015). United nations environment programme, global waste management outlook. http://www.unep.org/ietc/Portals/136/Publications/Waste%20Management/GWMO%20report/GWMO%20full%20report.pdf. Accessed on: April 19, 2016.

Van Schoor, M. (2002). Detection of sinkholes using 2d electrical resistivity imaging. *Journal of Applied Geophysics*, 50.

Vouillamoz, J. M., Legchenko, A., Albouy, Y., Bakalowicz, M., Baltassat, J. M., and Al-Fares, W. (2003). Localization of saturated karst aquifer with magnetic resonance sounding and resistivity imagery. *Groundwater*, 41(5):578–586.

Wemegah, D. D. (2015). *Integrated Geophysical Characterization of Municipal Solid Waste Disposal Sites in the Kumasi Metropolis*. PhD thesis, Kwame Nkrumah University of Science and Technology, Kumasi, Ghana.

Wemegah, D. D., Fiandaca, G., Auken, E., Menyeh, A., and Danour, S. K. (2014). Time-domain spectral induced polarization and magnetics for mapping municipal solid waste deposits in ghana. *Near Surface Geoscience: 20th European Meeting of Environmental and Engineering Geophysics Athens, Greece, 14-18 September 2014*.

World Bank (2013). Global waste on a pace to triple by 2100. http://www.worldbank.org/en/news/feature/2013/10/30/global-waste-on-pace-to-triple. Accessed on: March 13, 2016.

World Health Organisation (2006). Protecting groundwater for health: Managing the quality of drinking-water sources. Edited by O. Schmoll, G. Howard, J. Chilton and I. Chorus. ISBN: 1843390795. Published by IWA Publishing, London, UK.